ULTRAFAST DYNAMICS OF CARRIERS IN GERMANIUM PROBED BY BROADBAND FEMTOSECOND SPECTROSCOPIC ELLIPSOMETRY

Ph.D. dissertation defense

Carlos Antonio Armenta

July 9, 2025

Department of physics

BE BOLD. Shape the Future.®
New Mexico State University

Acknowledgments

- **Thesis advisor:**
  Dr. Stefan Zollner
- **Thesis committee**
  Dr. Igor Vasiliev
  Dr. Michael Engelhardt
  Dr. R. T. James McAteer
- **Research group (current)**
  Jaden R. Love
  Haley Woolf
  Sonam Yadav
  Yoshitha Hettige
  Aaron López
  Gabriel Ruiz
- **Research group (former)**
  Carola Emminger
  Nuwanjula Samarasingha
- **ELI Eric group**
  Dr. Shirly Espinoza
  Dr. Martín Zahradník
  Dr. Mateusz Rebarz
  Dr. Saul Vázquez-Miranda
  Dr. Jakob Andreasson
- **Arizona State University**
  Dr. José Menéndez
- **Funding agencies**
  Air Force Office of Scientific Research under award number FA9550-20-1-0135 and FA9453-23-2-0001.
  Department of Energy, National Nuclear Security Administration under award number DE-NA0004103.
  National Science Foundation under award number DMR-2423992.
  J. A. Woollam foundation.

Vita

Publications

1) M. R. Arias, C. A. Armenta, C. Emminger, C. M. Zamarripa, N. S. Samarasingha, J. R. Love, S. Yadav, and S. Zollner, J. Vac. Sci. Technol. B **41**, 022203 (2023).

2) C. A. Armenta, M. Zahradník, M. Rebarz, C. Emminger, S. Espinoza, S. Vazquez-Miranda, J. Andreasson, and S. Zollner, 2024 IEEE Photonics Society Summer Topicals Meeting Series (SUM), Bridgetown, Barbados, 2024, pp. 01-02.

3) S. Zollner, C. A. Armenta, S. Yadav, and J. Menéndez, J. Vac. Sci. Technol. A **43**, 012801 (2025).

4) C. A. Armenta and S. Zollner, J. Appl. Phys. **137**, 245701 (2025).

5) C. A. Armenta, M. Zahradník, M. Rebarz, C. Emminger, S. Espinoza, S. Vazquez-Miranda, J. Andreasson, and S. Zollner, (in preparation).

Oral presentations

- AVS 68th International Symposium & Exhibit. Pittsburgh, PA, November 8, 2022.
- APS March Meeting 2023, Las Vegas, NV, March 7, 2023.
- 12th Workshop on Spectroscopic Ellipsometry. Prague, Czech Republic, September 19, 2023
- AVS 69th International Symposium & Exhibit. Portland, OR, November 6, 2023.
- IEEE 2024 Summer Topical Meeting Series. Bridgetown, Barbados, July 16, 2024.
- LXVI Congreso Nacional de Física. Chihuahua, México, October 9, 2024.
- AVS 70th International Symposium & Exhibit. Tampa, FL, November 8, 2024.
- 10th International Conference on Spectroscopic Ellipsometry. Boulder, CO, June 13, 2024.
- **Invited talk**: AVS 71st International Symposium & Exhibit. Charlotte, NC, September 21, 2025.

Future position: IBM Research

Outline

- **Introduction**
  - Problem statement
  - Dielectric function range
- **Steady-state dielectric function**
  - Critical points E_1 and E_1+Δ_1
  - Excitons
  - Spectroscopic ellipsometry
  - Results
- **Ultrafast dynamics**
  - Femtosecond ellipsometry
  - Scattering and relaxation of carriers
  - Carrier statistics
- **Modeling of dielectric function**
- **Fit of data**
- **Conclusion**

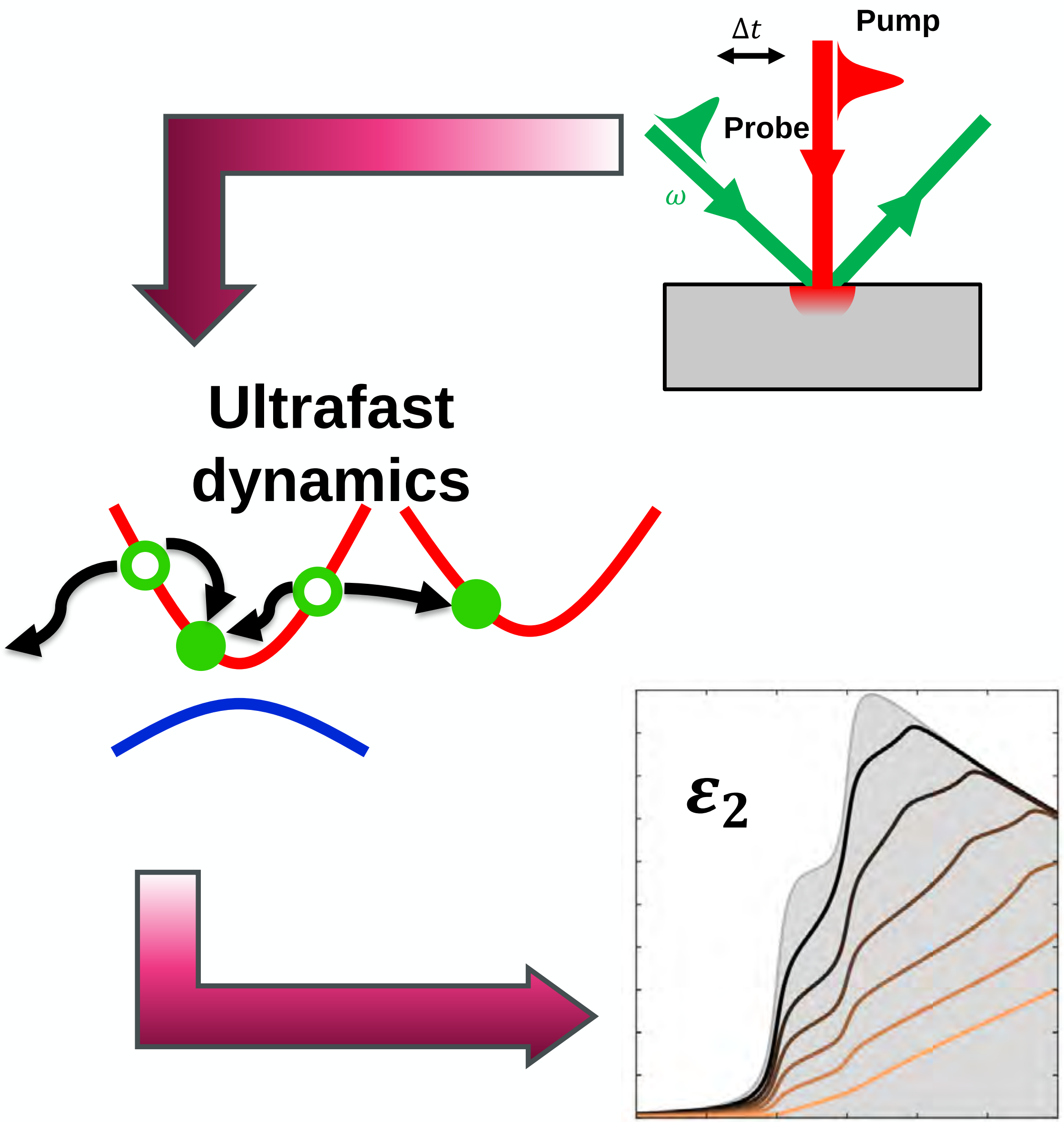

Introduction

BE BOLD. Shape the Future.®
New Mexico State University

Problem statement

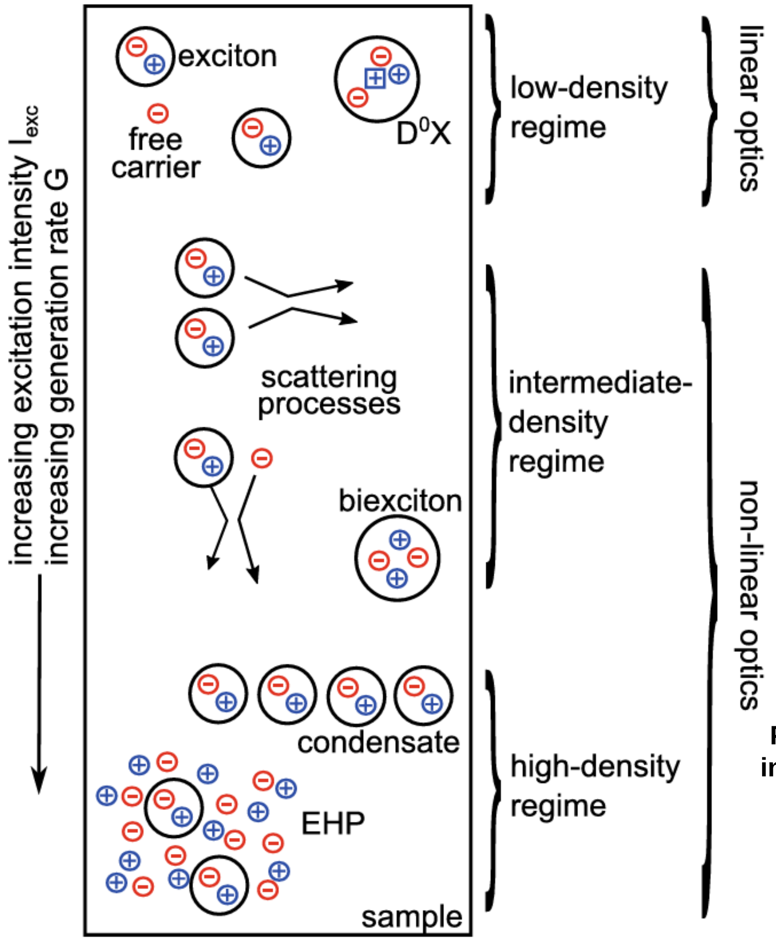

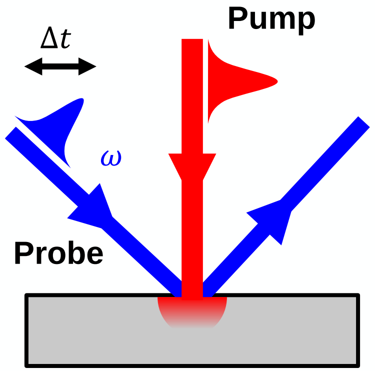

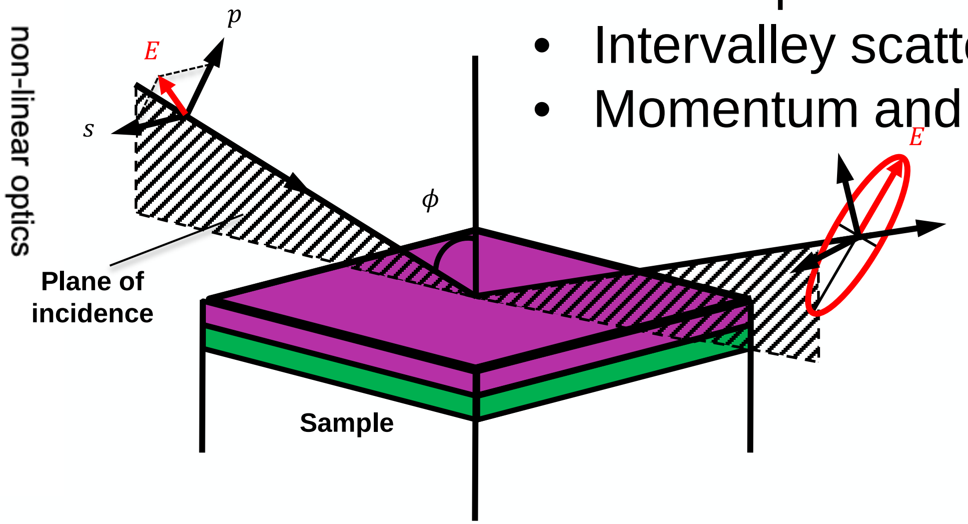

The study of non-linear effects in germanium induced by photoexcited carriers by using time resolve ellipsometry:

- Carrier-carrier scattering.
- Carrier-phonon scattering.
- Intervalley scattering.
- Momentum and energy relaxation of hot carriers.

NM STATE BE BOLD. Shape the Future.®

H. Kalt, C. F. Klingshirn, *Semiconductor Optics 2* (Springer, 2024).
H. G. Tompkins and J. N. Hilfiker, *Spectroscopic Ellipsometry* (Momentum Press, 2016).

Dielectric function of Ge

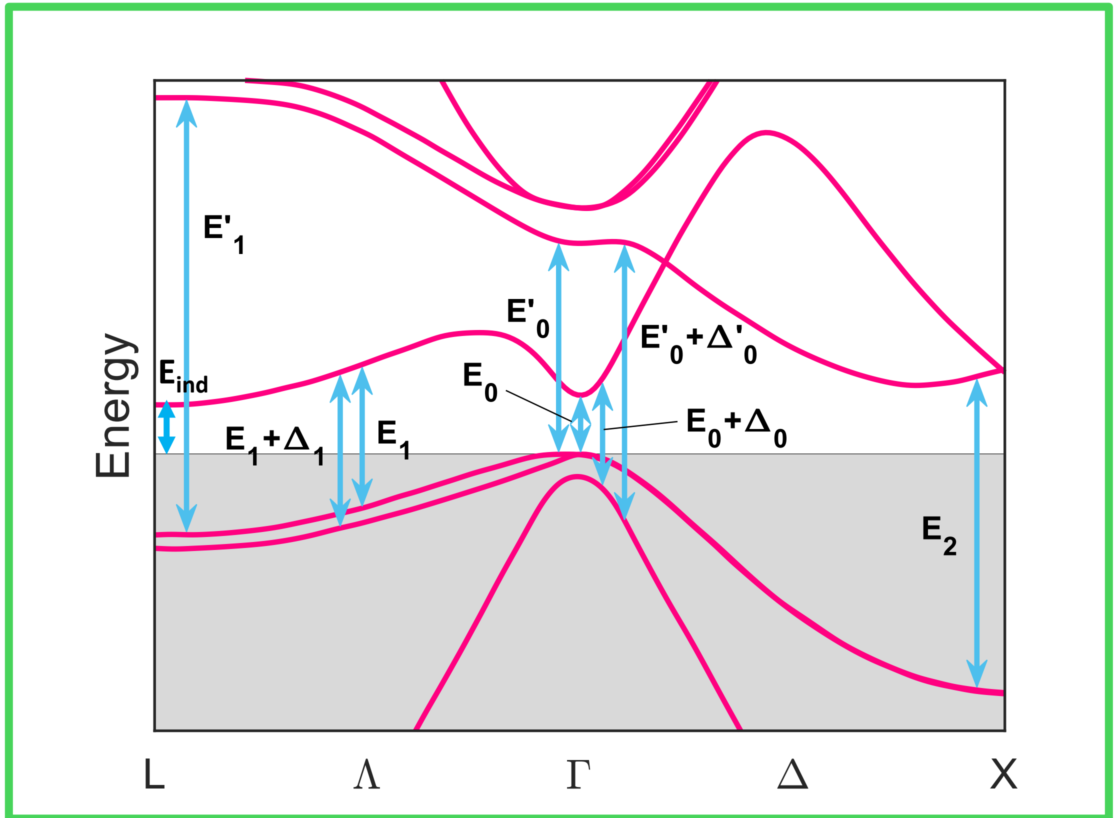

Band Structure of Ge

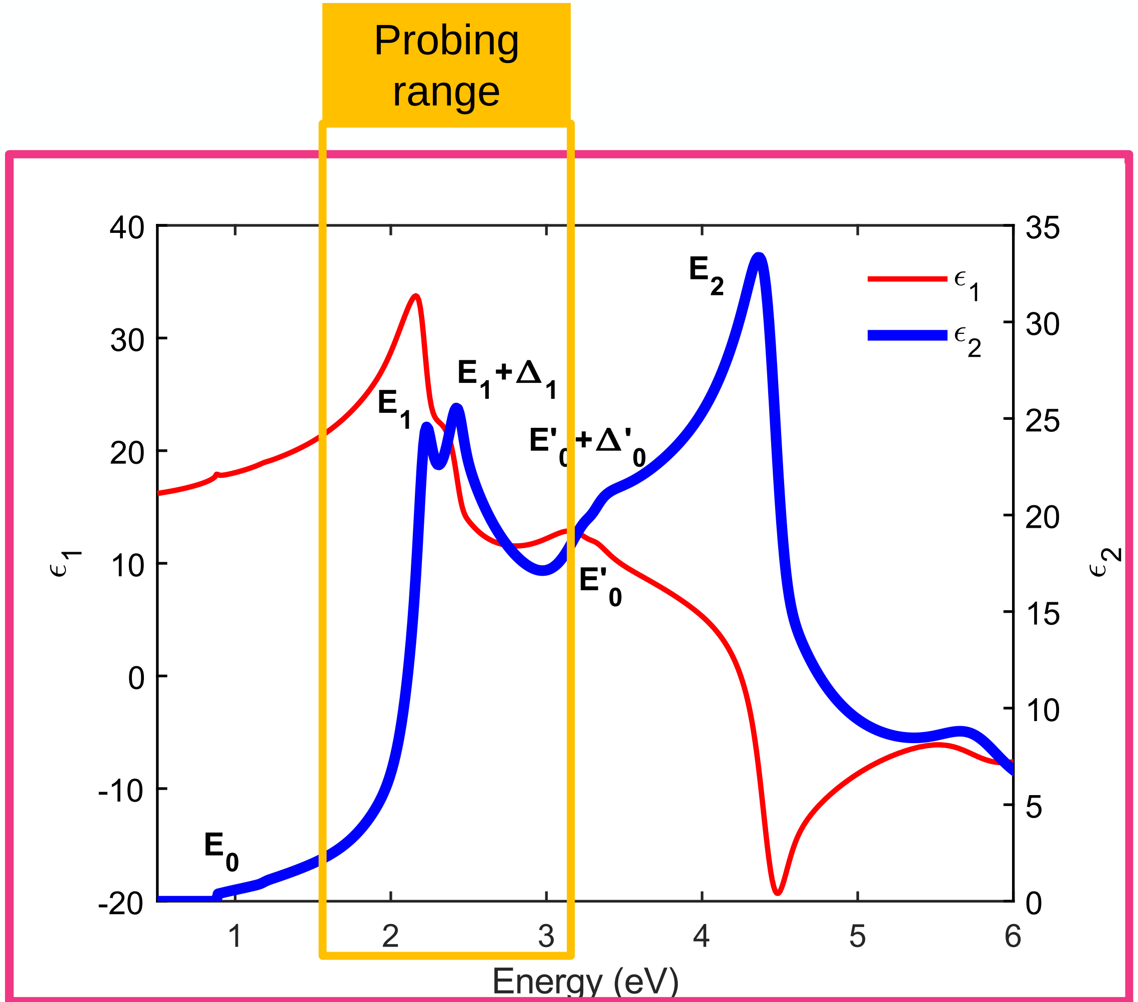

Dielectric Function of Ge

Critical points when the JDOS becomes singular

$$J_{CV}(E) \propto \int \frac{\mathrm{d}\mathbf{S}}{|\nabla_{\mathbf{k}}[E_C(\mathbf{k}) - E_V(\mathbf{k})]|}$$

NM STATE BE BOLD. Shape the Future.®

P. Yu and M. Cardona, *Fundamentals of Semiconductors* (Springer, Berlin, 1996).
C. Emminger *et al.*, J. Vac. Sci. Technol. B **38**, 012202 (2020).

Steady state dielectric function

BE BOLD. Shape the Future.®
New Mexico State University

Dielectric function of Ge

- The shape of the dielectric function near the critical points E_1 and $E_1+\Delta_1$ requires a better description.
- Existing *ab initio* expressions are inadequate due to the omission of excitonic effects.
- Recent efforts that employ more sophisticated techniques are still not ideal.
- A closed form model can help us understand other physics such as ultrafast phenomena.

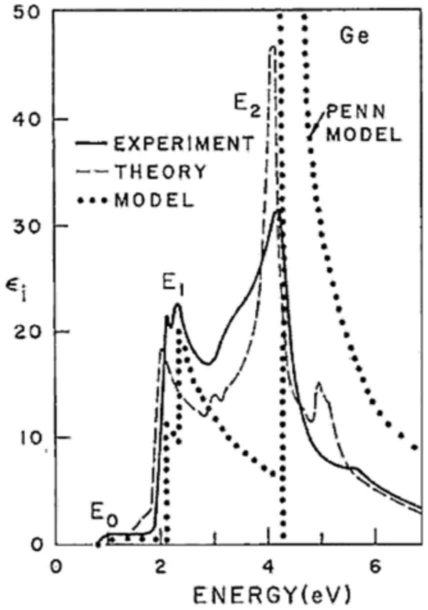

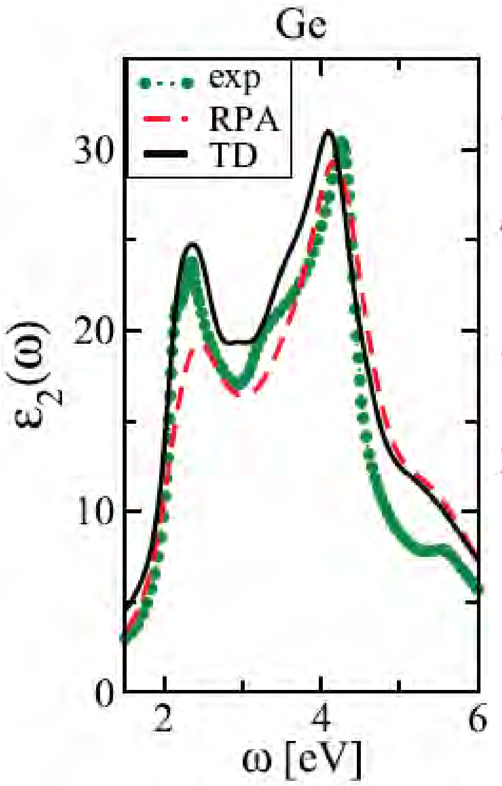

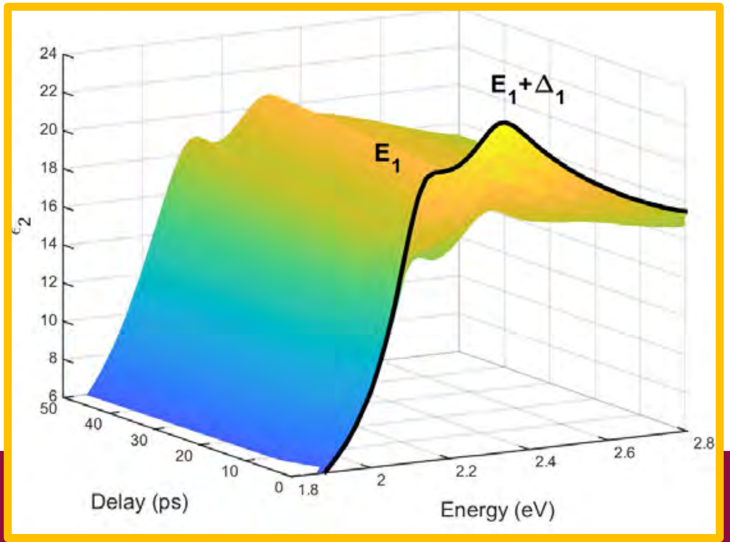

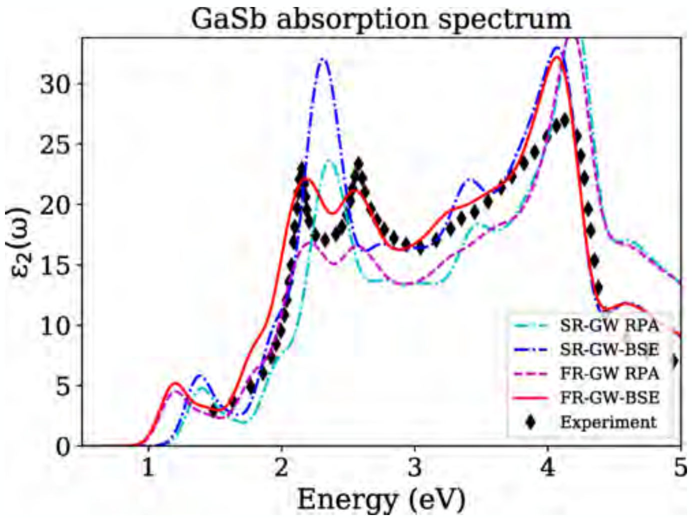

NM STATE BE BOLD. Shape the Future.®

M. Cardona and F. H. Pollak, in *The Physics of Optoelectronic Materials,* edited by W. Alberts (Academic, New York 1971), p. 81.
P. E. Trevisanutto *et al.*, Phys. Rev. B **87**, 205143 (2013).
B. A. Barker *et al.*, Phys. Rev. B **106**, 115127 (2022).

E_1 and $E_1+\Delta_1$ critical points

2D van Hove singularities

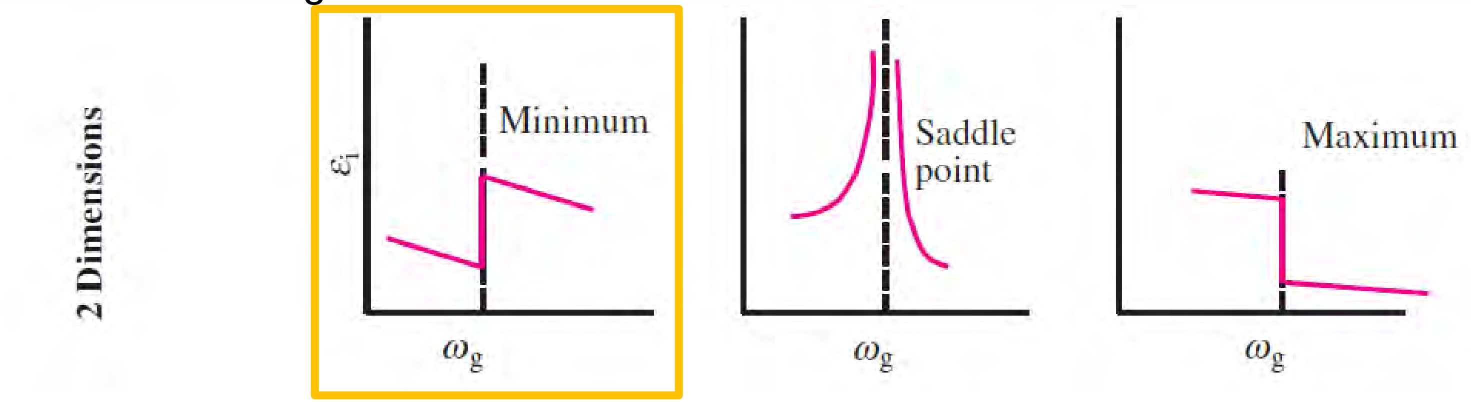

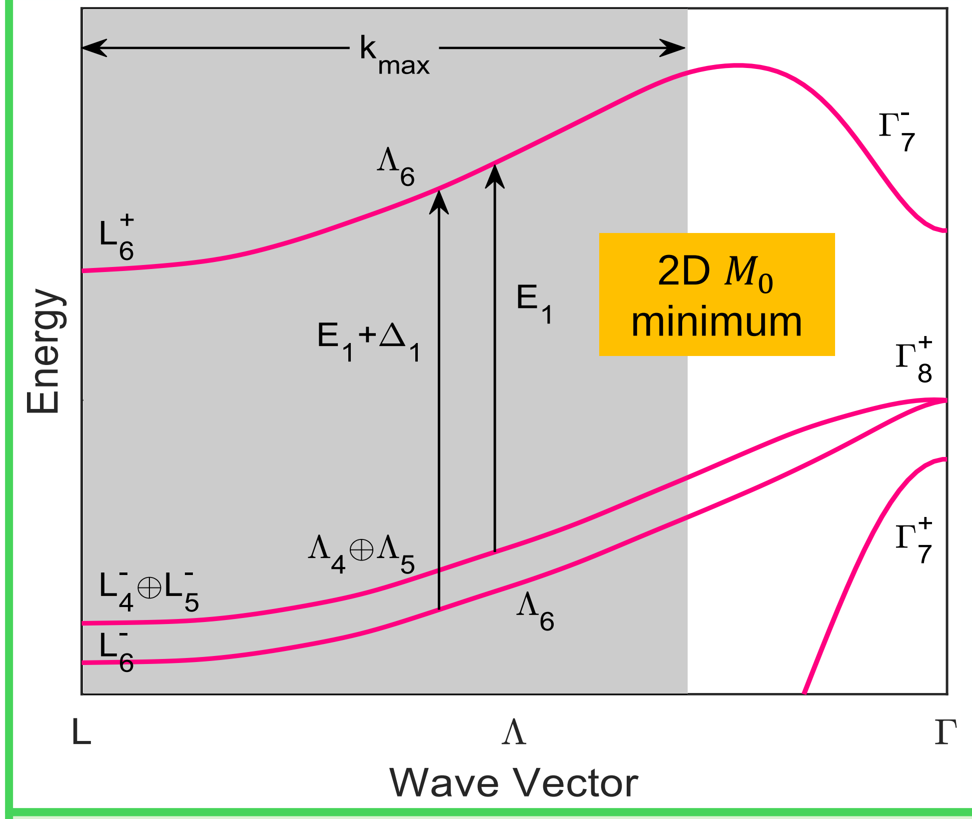

In the parabolic approximation and with bands at the L-valley (L_6^+ and $L_4^- \oplus L_5^-$), the dielectric function in cylindrical coordinates is

$$\varepsilon_2(E) = \left(\frac{1}{4\pi\varepsilon_0}\right)\frac{4\pi^2 e^2\hbar^2\bar{P}^2}{3m_0^2E^2}\iiint \frac{k_\rho \mathrm{d}k_\rho \mathrm{d}k_\varphi \mathrm{d}k_z}{4\pi^3}\,\delta\left[E_1 + \frac{\hbar^2k_\rho^2}{2\mu_\perp} + \frac{\hbar^2k_z^2}{2\mu_\parallel} - E\right]$$

Now we integrate up to the value in the BZ where $\mu_\parallel \to \infty$ holds (k_{max}). We also multiply by the valley degeneracy (4 for the L-valley).

$$\varepsilon_2^{(E_1)}(E) = \left(\frac{1}{4\pi\varepsilon_0}\right)\frac{16e^2\bar{P}^2\mu_\perp k_{\mathrm{max}}}{3m_0^2E^2}H(E_1 - E)$$

Without broadening!

Kramers-Kronig transformation:

$$\varepsilon_1^{(E_1)}(E) = -\left(\frac{1}{4\pi\varepsilon_0}\right)\frac{16e^2\bar{P}^2\mu_\perp k_{\mathrm{max}}}{3m_0^2E^2}\ln\left(\frac{E_1^2 - E^2}{E_1^2}\right)$$

P. Yu and M. Cardona, *Fundamentals of Semiconductors* (Springer, Berlin, 1996).
M. Cardona, in *Atomic Structure and Properties of Solids,* edited by E. Burstein (Academic, New York, 1972), p. 514.

Wannier excitons

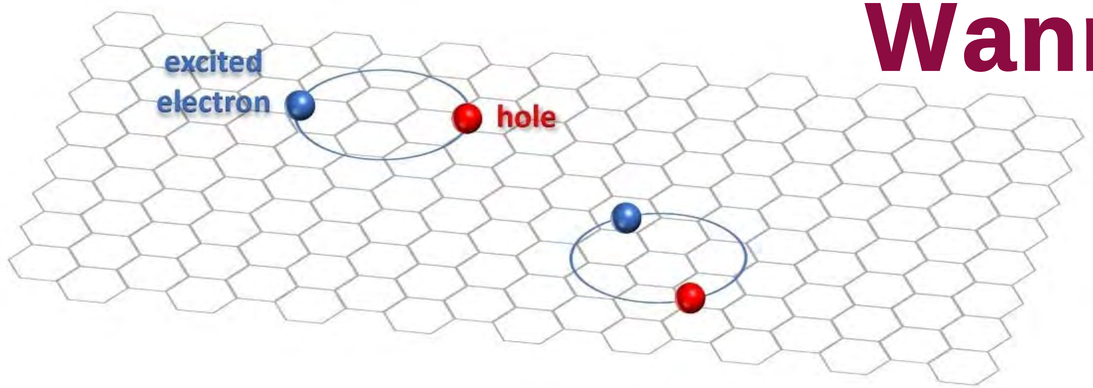

Dispersion relation of the excitons:

$$\begin{cases} E_{\text{ex}} = E_g - \dfrac{R}{n^2} + \dfrac{\hbar^2 \vec{K}^2}{2M} \\ M = m_e + m_h \\ \dfrac{1}{\mu} = \dfrac{1}{m_e} + \dfrac{1}{m_h} \\ \vec{K} = \vec{k}_e + \vec{k}_h \end{cases}$$

The formation of a quasi-particle of an electron and a hole bound together in a hydrogen-like system.

$$\varepsilon_2^{(3\text{D})}(E) = \frac{A}{E^2}\left[\underbrace{\sum_{n=1}^{\infty} \frac{4\pi R^{3/2}}{n^3}\,\delta\!\left(E - E_g + \frac{R}{n^2}\right)}_{\text{Discrete}} + \underbrace{\frac{2\pi\sqrt{R}\,H(E - E_g)}{1 - e^{-2\pi\sqrt{R/(E-E_g)}}}}_{\text{Continuum}}\right]$$

$$\varepsilon_2^{(2\text{D})}(E) = \frac{A}{E^2}\left[\underbrace{\sum_{n=0}^{\infty} \frac{4R}{(n+1/2)^3}\,\delta\!\left(E - E_g + \frac{R}{(n+1/2)^2}\right)}_{\text{Discrete}} + \underbrace{\frac{2H(E - E_g)}{1 - e^{-2\pi\sqrt{R/(E-E_g)}}}}_{\text{Continuum}}\right]$$

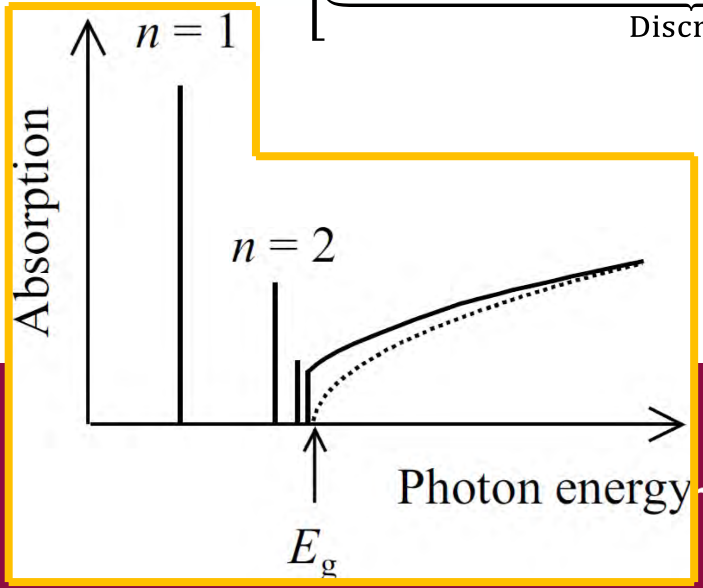

Binding energy of the exciton:

$$R^{(3\text{D})} = \frac{\mu}{\varepsilon_{\text{st}}^2}\,\text{Ry}$$

$$R^{(2\text{D})} = \frac{4\mu}{\varepsilon_{\text{st}}^2}\,\text{Ry}$$

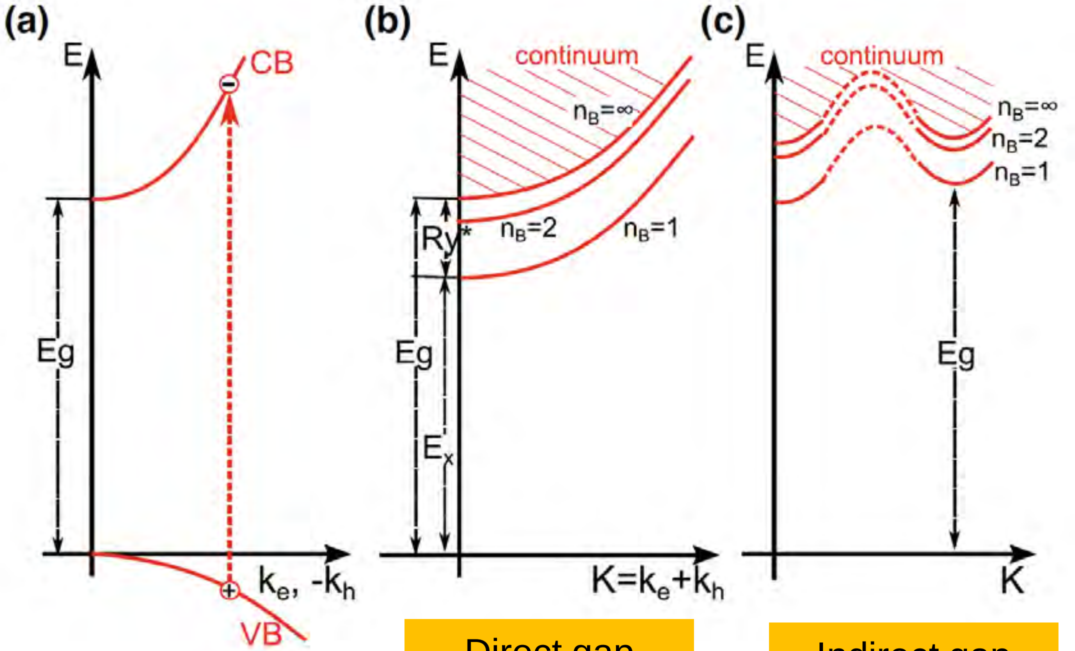

Direct gap Semiconductor

Indirect gap Semiconductor

R. J. Elliot, Phys. Rev. **108**, 1384 (1957).
M. Shinado & S. Sugano, J. Phys. Soc. Jpn. **21**, 1936 (1966).
H. Kalt, C. F. Klingshirn, *Semiconductor Optics 1* (Springer, 2019).

2D Excitons

2D JDOS:

$$E_{\mathrm{CV}}\left(\vec{k}\right) = E_g + \frac{\hbar^2}{2}\left(\frac{k_x^2 + k_y^2}{\mu_\perp} + \cancelto{0}{\frac{k_z^2}{\mu_\parallel}}\right)$$

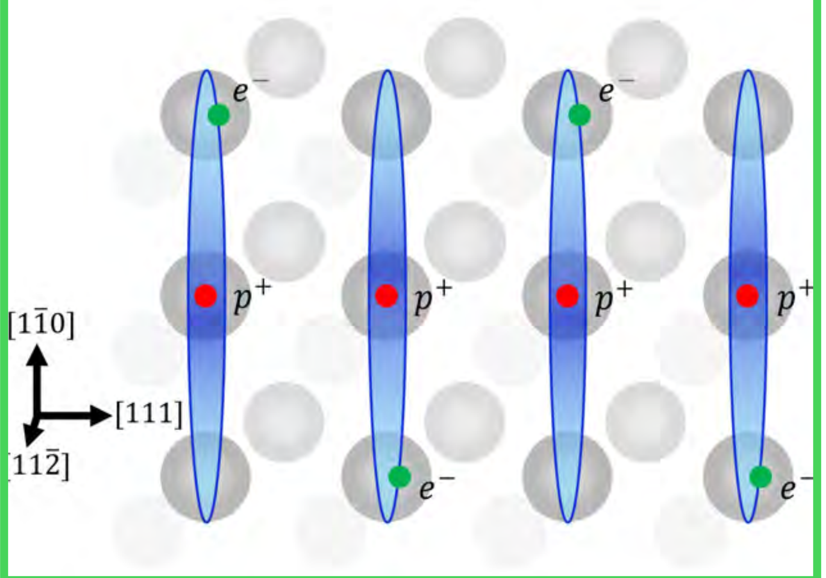

Binding energy:

$$R = \frac{4\mu_\perp}{\varepsilon_{\mathrm{st}}^2}\mathrm{Ry}$$

Adding broadening to the uncorrelated electron-hole pair DF:

$$\varepsilon^{\mathrm{un}}(E) = \frac{A^{(E_g)}}{E^2}\ln\left[\frac{2\left(E_g - i\Gamma - E\right)}{E_g - i\Gamma}\right]$$

Tanguy 2D exciton DF:

$$\varepsilon^{2\mathrm{D}}(E) = \frac{A^{(E_g)}}{\pi(E + i\Gamma)^2}\{g_a[\xi(E + i\Gamma)] + g_a[\xi(E + i\Gamma)] - 2g_a[\xi(0)]\}$$

$$\xi(z) = \sqrt{R/(E_g - z)}, \qquad g_a(\xi) = 2\ln\xi - 2\psi(1/2 - \xi)$$

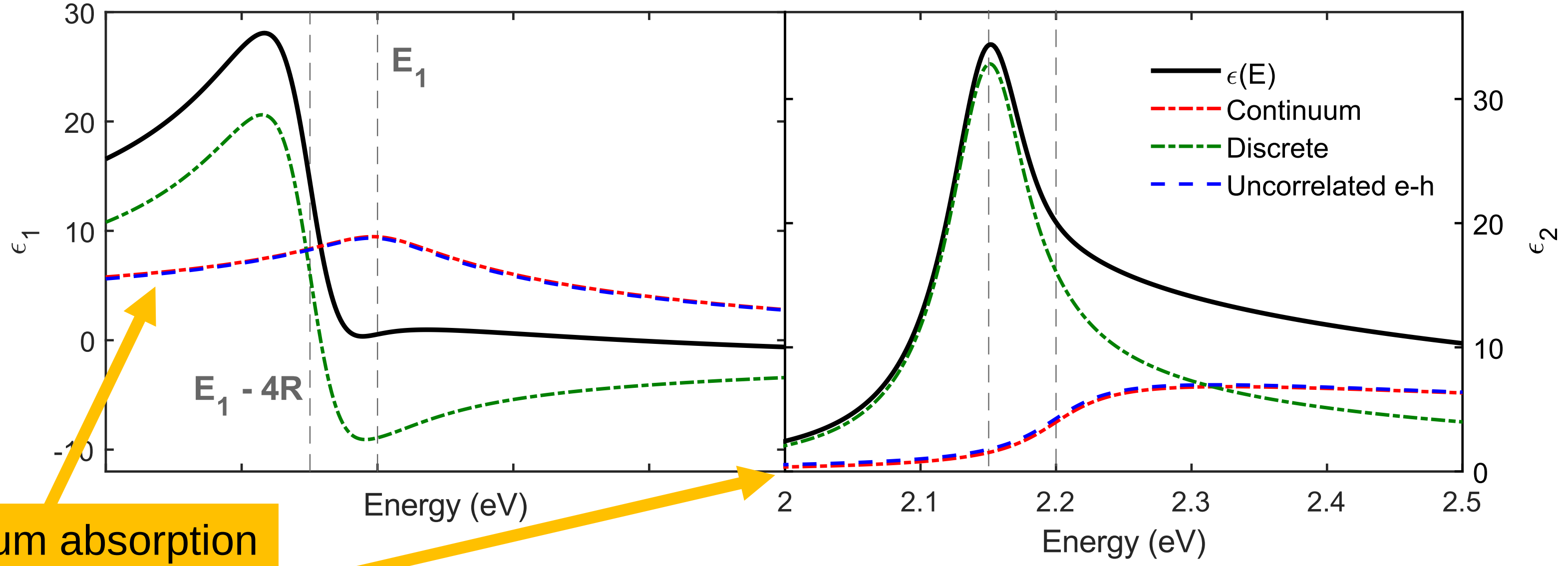

Continuum absorption and uncorrelated e-h overlap.

J, Humlíček, Phys. Stat. Solid. (b) **77**, 731 (1976).
C. Tanguy, Solid State Commun. **98**, 65 (1996).

NM STATE BE BOLD. Shape the Future.®

Amplitude and binding energy

Reduced masses come from a 6 band $\mathbf{k}\cdot\mathbf{p}$-theory model.

The amplitude for the critical points are:

$$A^{(E_1)} = \frac{4e^2\bar{P}^2\mu_\perp^{(E_1)}k_{\max}}{3\pi\varepsilon_0 m_0^2}, \qquad A^{(E_1+\Delta_1)} = \frac{4e^2\bar{P}^2\mu_\perp^{(E_1+\Delta_1)}k_{\max}}{3\pi\varepsilon_0 m_0^2}$$

In the parabolic approximation

$$\frac{1}{\mu_\perp^{(E_1)}} = \frac{\bar{P}^2}{m_0}\left[\frac{2}{E_1^u} + \frac{1}{(E_1+\Delta_1)^u}\right], \qquad \frac{1}{\mu_\perp^{(E_1+\Delta_1)}} = \frac{\bar{P}^2}{m_0}\left[\frac{1}{E_1^u} + \frac{2}{(E_1+\Delta_1)^u}\right]$$

and amplitudes are

$$A^{(E_1)} = \frac{4e^2E_1^u(E_1+\Delta_1)^u k_{\max}}{3\pi\varepsilon_0[2E_1^u(E_1+\Delta_1)^u + E_1^u]}$$

$$A^{(E_1+\Delta_1)} = \frac{4e^2E_1^u(E_1+\Delta_1)^u k_{\max}}{3\pi\varepsilon_0[E_1^u(E_1+\Delta_1)^u + 2E_1^u]}$$

We must use unrenormalized energy

$$E^u_{E_1,E_1+\Delta_1}(T) = E^{\exp}_{E_1,E_1+\Delta_1}(0\ \mathrm{K}) - 3B\left(\frac{\partial E^{\exp}_{E_1,E_1+\Delta_1}}{\partial p}\right)_T \int_0^T \alpha(\theta)\mathrm{d}\theta$$

Thermal expansion coefficient $\alpha(T)$

$$\alpha(T) = \frac{1}{a_0(T)}\frac{\mathrm{d}a_0(T)}{\mathrm{d}T}.$$

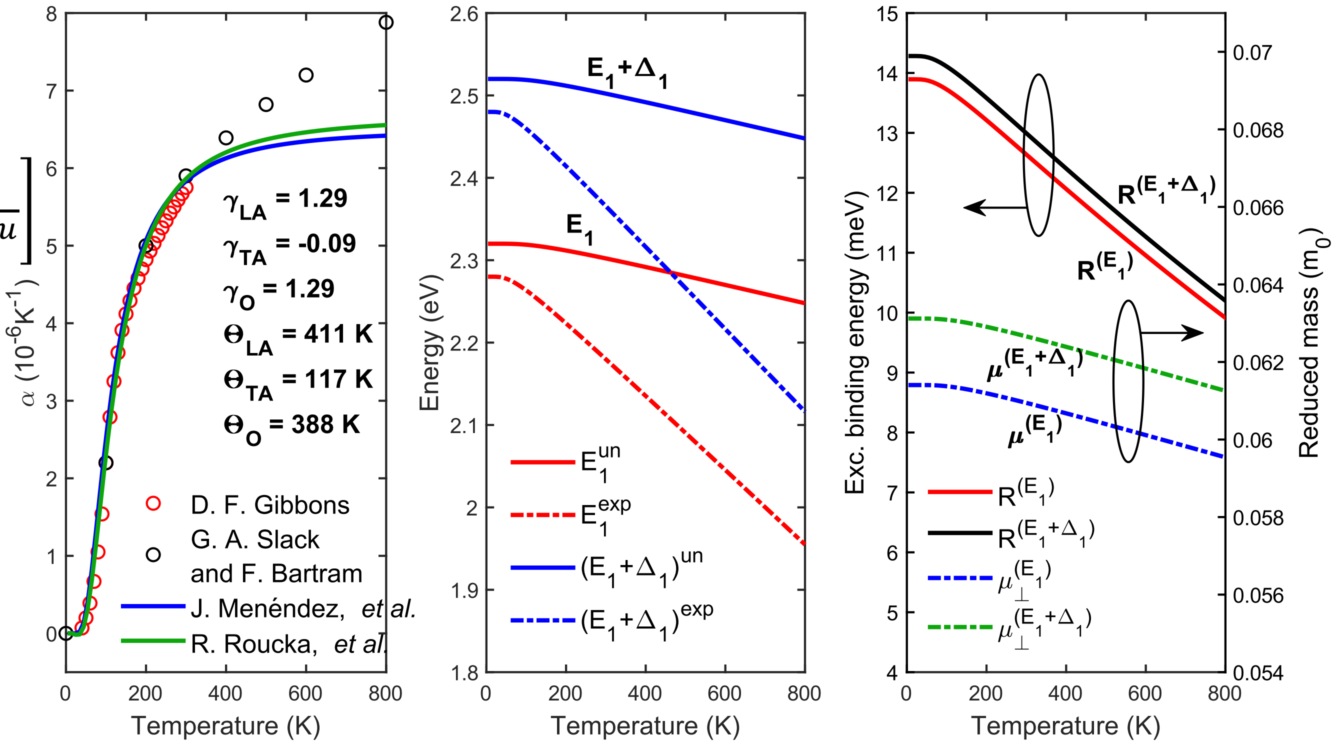

Binding energy of the exciton:

$$R = \frac{4\mu_\perp^u}{\varepsilon_{\mathrm{st}}^2(T)}\mathrm{Ry}$$

C. Emminger *et al.*, J. Appl. Phys. **131**, 165701 (2022).
S. Zollner *et al.*, J. Vac. Sci. Technol. A **43**, 012801 (2025).
J. Menéndez *et al.*, Phys. Rev. B **98**, 165207 (2018).
R. Roucka *et al.*, Phys. Rev. B **81**, 245214 (2010).

Experimental data & results

BE BOLD. Shape the Future.®
New Mexico State University

Spectroscopic ellipsometry

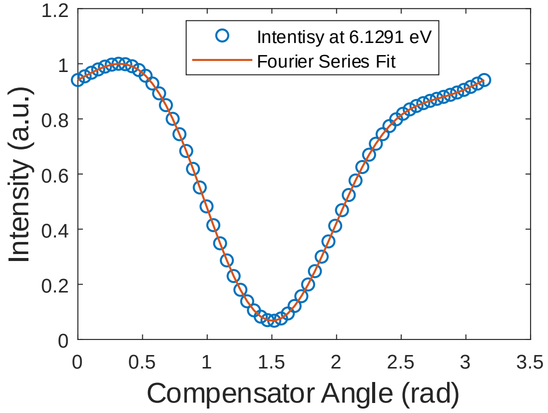

Fundamental equation of ellipsometry:

$$\rho = \tan\Psi e^{i\Delta} = \frac{r_\mathrm{p}}{r_\mathrm{s}}$$

Complex pseudo-dielectric function:

$$\langle\varepsilon\rangle = \sin^2\theta\left[1 + \tan^2\theta\left(\frac{1-\rho}{1+\rho}\right)\right]$$

Fresnel equations:

$$r_\mathrm{p} = \frac{\varepsilon\cos\theta - (\varepsilon - \sin^2\theta)^{1/2}}{\varepsilon\cos\theta + (\varepsilon - \sin^2\theta)^{1/2}}$$

$$r_\mathrm{s} = \frac{\cos\theta - (\varepsilon - \sin^2\theta)^{1/2}}{\cos\theta + (\varepsilon - \sin^2\theta)^{1/2}}$$

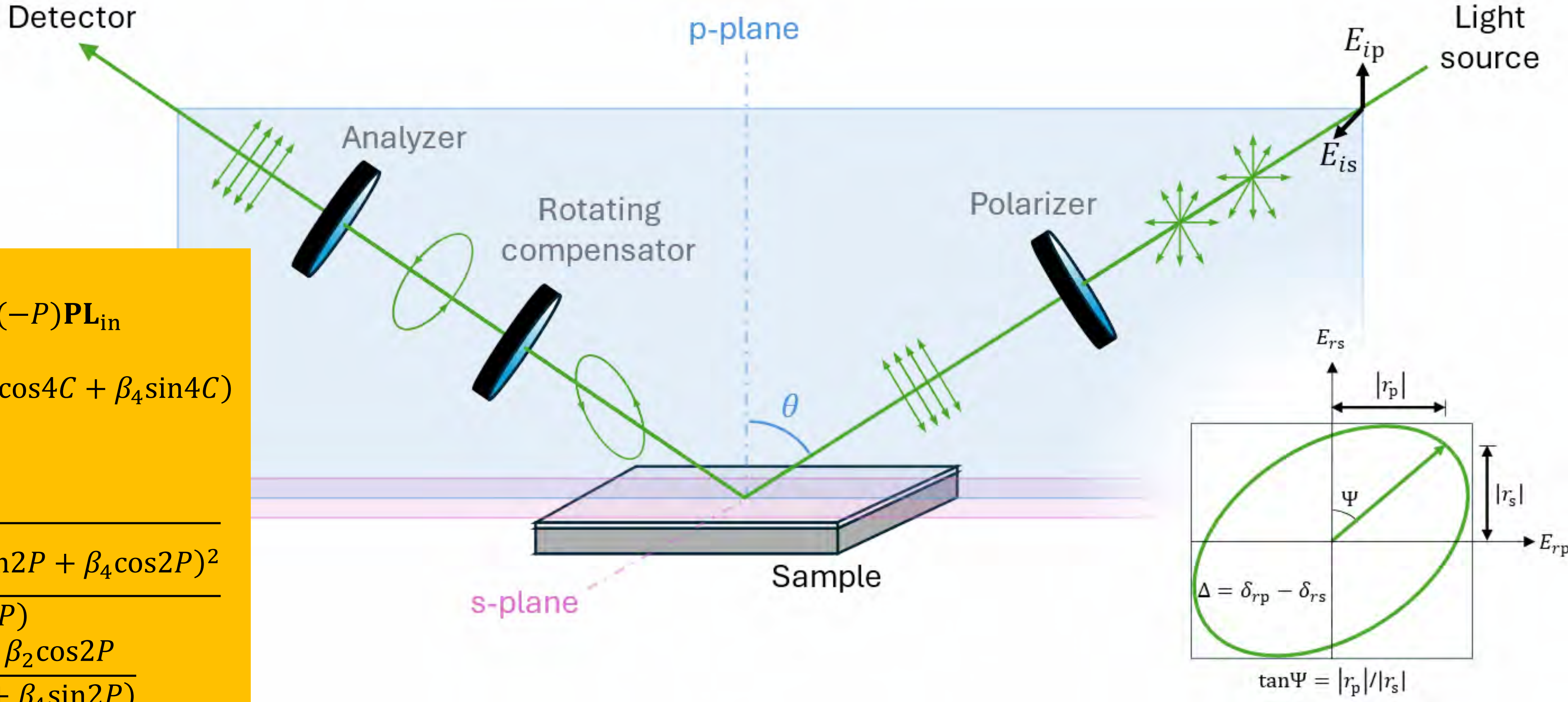

RCE in Jones matrix/vector formalism:

$$\mathbf{L}_\mathrm{out} = \mathbf{A}\mathbf{R}(-A)\mathbf{R}(C)\mathbf{C}\mathbf{R}(-C)\mathbf{S}\mathbf{R}(-P)\mathbf{P}\mathbf{L}_\mathrm{in}$$

$$I(C) = I_0(\alpha_0 + \alpha_2\cos 2C + \beta_2\sin 2C + \alpha_4\cos 4C + \beta_4\sin 4C)$$

Ellipsometric angles:

$$\tan 2\Psi = -\frac{\sqrt{\dfrac{(\alpha_2^2+\beta_2^2)(1-\cos\delta)^2}{\sin^2\delta} + 4(-\alpha_4\sin 2P + \beta_4\cos 2P)^2}}{2(\alpha_4\cos 2P + \beta_4\sin 2P)}$$

$$\tan 2\Delta = \left(\frac{1-\cos\delta}{2\sin\delta}\right)\frac{\alpha_2\sin 2P - \beta_2\cos 2P}{2(\alpha_4\cos 2P + \beta_4\sin 2P)}$$

H. Fujiwara, *Spectroscopic Ellipsometry* (John Wiley & Sons, 2007).
R. Kleim *et al.*, J. Opt. Soc. Am. A **11**, 2550 (1994).

2nd Derivative fit

To fit energy and broadening, we performed a 2nd derivative analysis with a Savitzky-Golay and extended Gaussian digital filter.

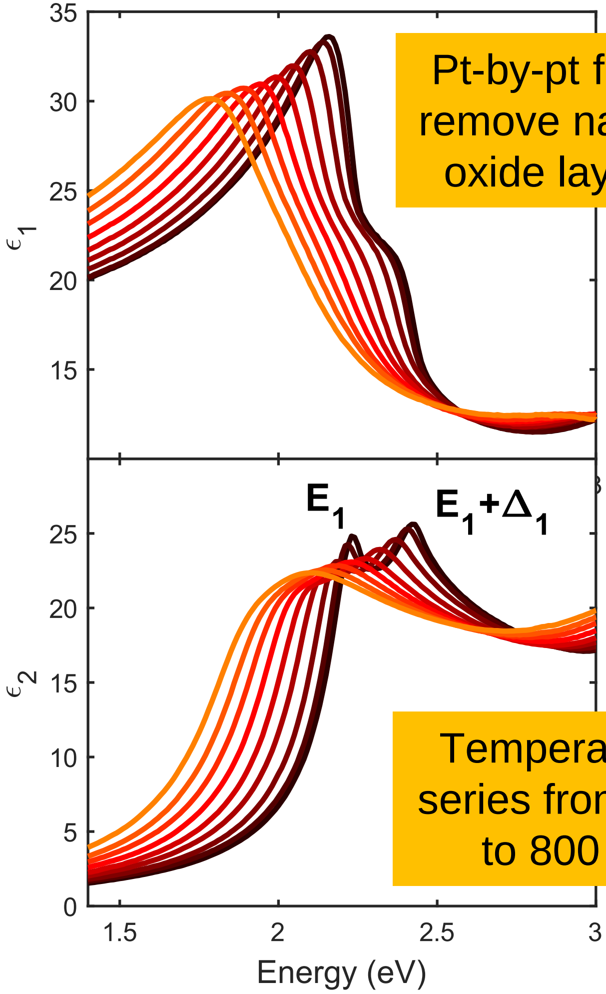

Pt-by-pt fit to remove native oxide layer.

Temperature series from 4 K to 800 K

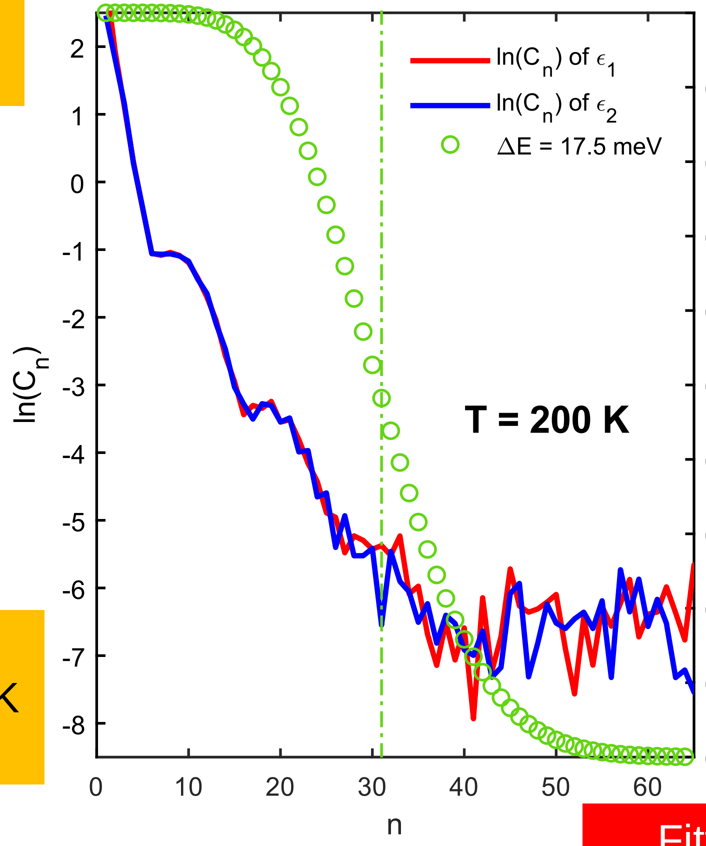

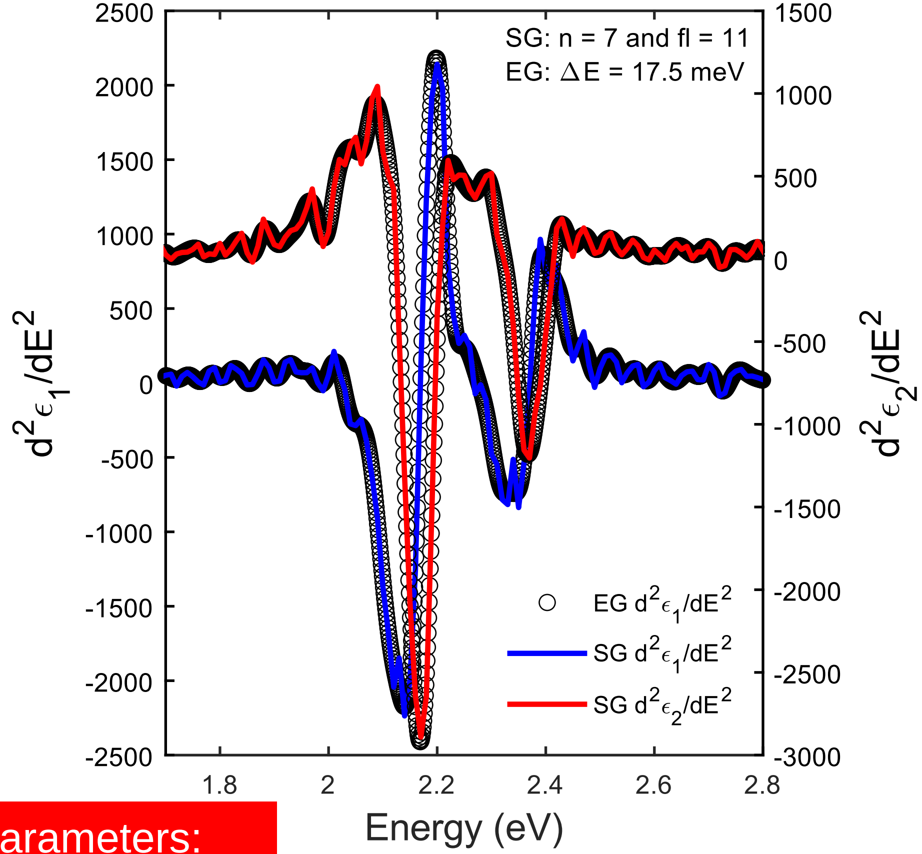

Fitting parameters:
$$\left[E_1, \Delta_1, \Gamma^{(E_1)}, \Gamma^{(E_1+\Delta_1)}, \varepsilon_{\text{off}}\right]$$

BE BOLD. Shape the Future.®

C. Emminger *et al.*, J. Vac. Sci. Technol. B **38**, 012202 (2020).
T. N. Nunley *et al.*, J. Vac. Sci. Technol. B **34**, 061205 (2016).
V. L. Le *et al.*, J. Vac. Sci. Technol. B **37**, 052903 (2019).
A. Savitzky and M. J. E. Golay, Anal. Chem. **36**, 1627 (1964).

2^{nd} Derivative fit

To fit energy and broadening, we performed a 2^{nd} derivative analysis with a Savitzky-Golay and extended Gaussian digital filter.

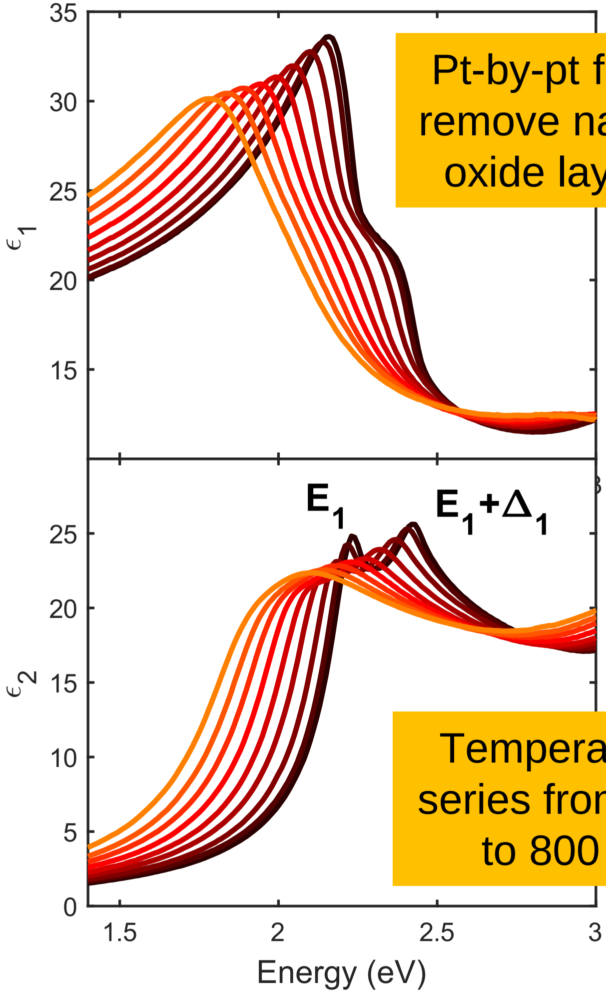

Pt-by-pt fit to remove native oxide layer.

Temperature series from 4 K to 800 K

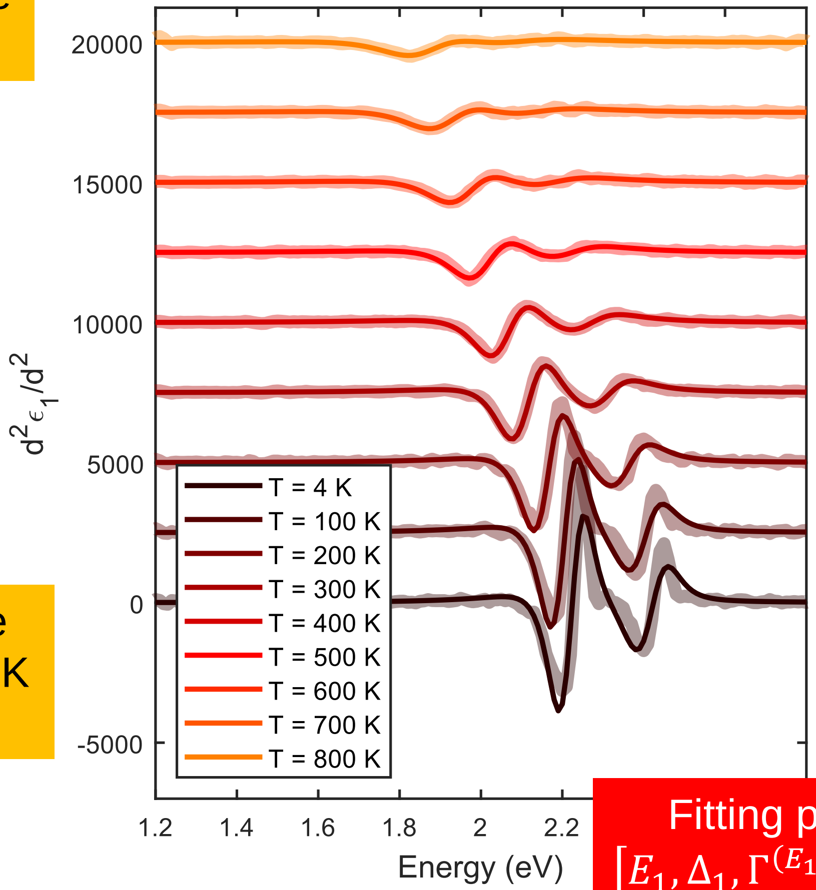

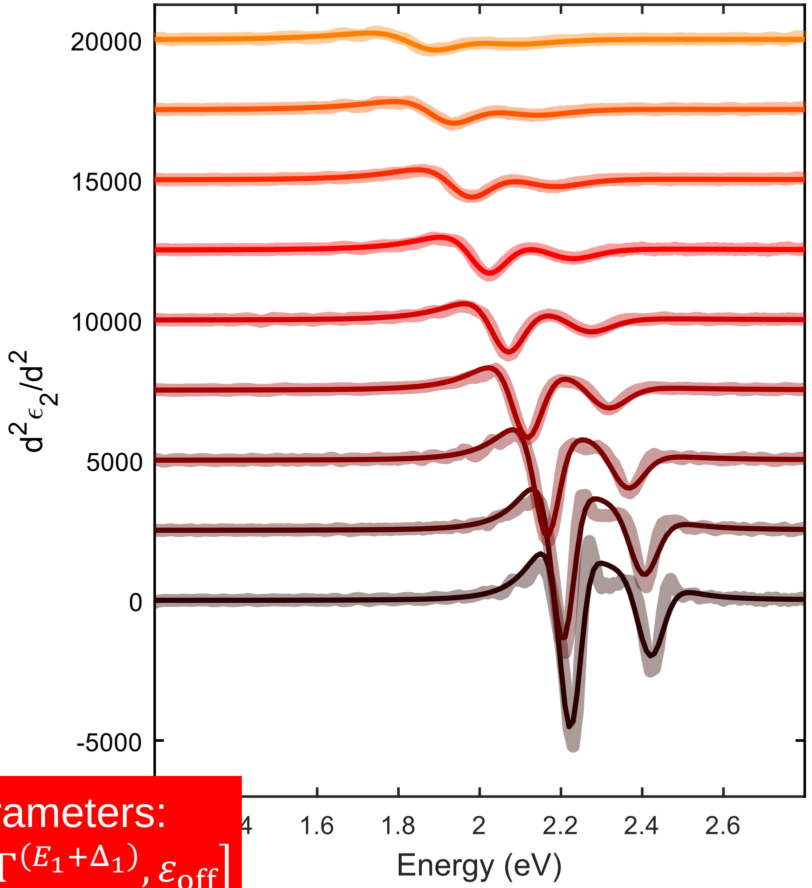

Fitting parameters:

$$\left[E_1, \Delta_1, \Gamma^{(E_1)}, \Gamma^{(E_1+\Delta_1)}, \varepsilon_{\text{off}}\right]$$

NM STATE BE BOLD. Shape the Future.®

C. Emminger *et al.*, J. Vac. Sci. Technol. B **38**, 012202 (2020).
T. N. Nunley *et al.*, J. Vac. Sci. Technol. B **34**, 061205 (2016).
V. L. Le *et al.*, J. Vac. Sci. Technol. B **37**, 052903 (2019).

Dielectric function

Offset added to the real part to account for additional CPs

Amplitude of ε_2 at E_1 is underestimated, whereas for $E_1+\Delta_1$ is overestimated.

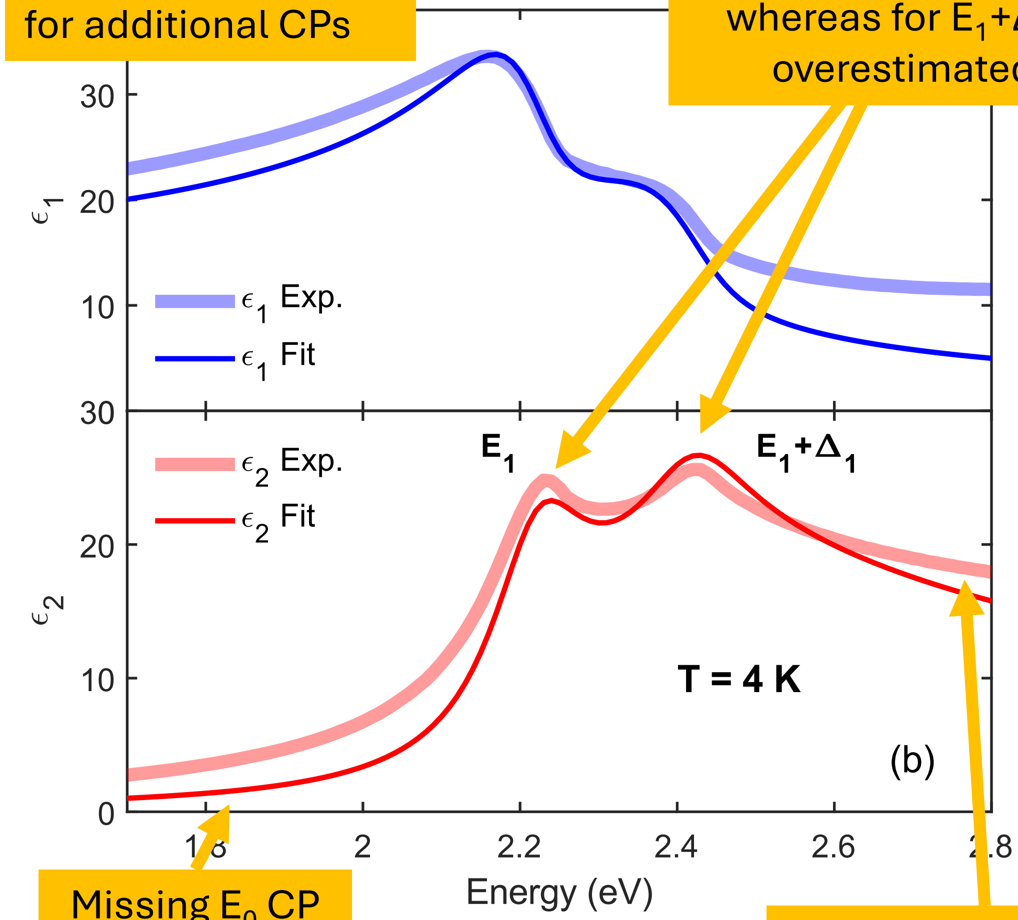

Missing E_0 CP at low energies

Missing E_0' and E_2 CPs at high energies

Maximum absorption occurs at $E_1 - 4R$.

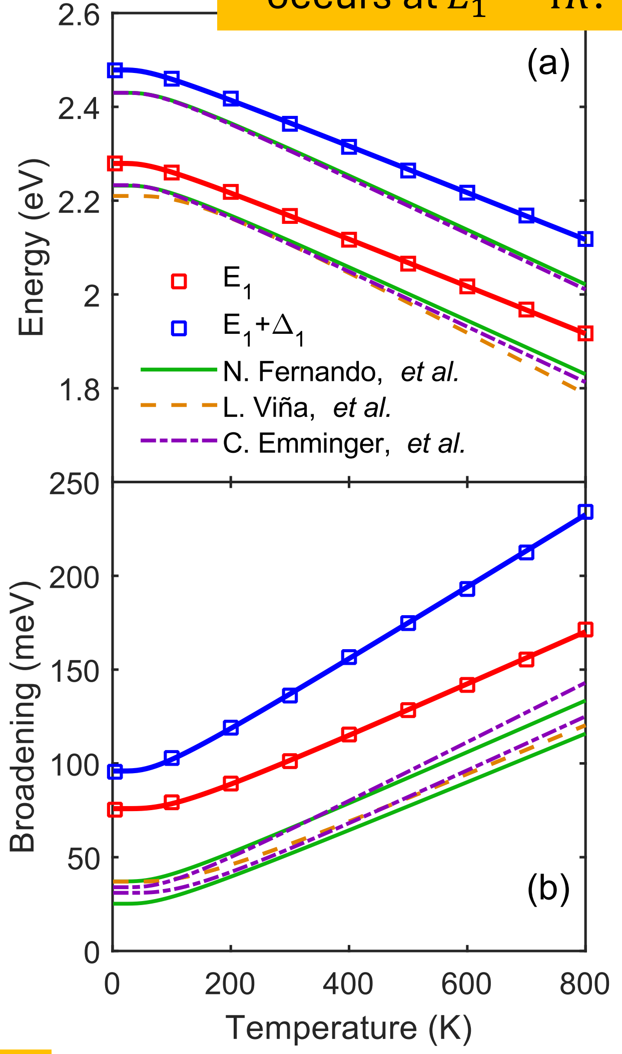

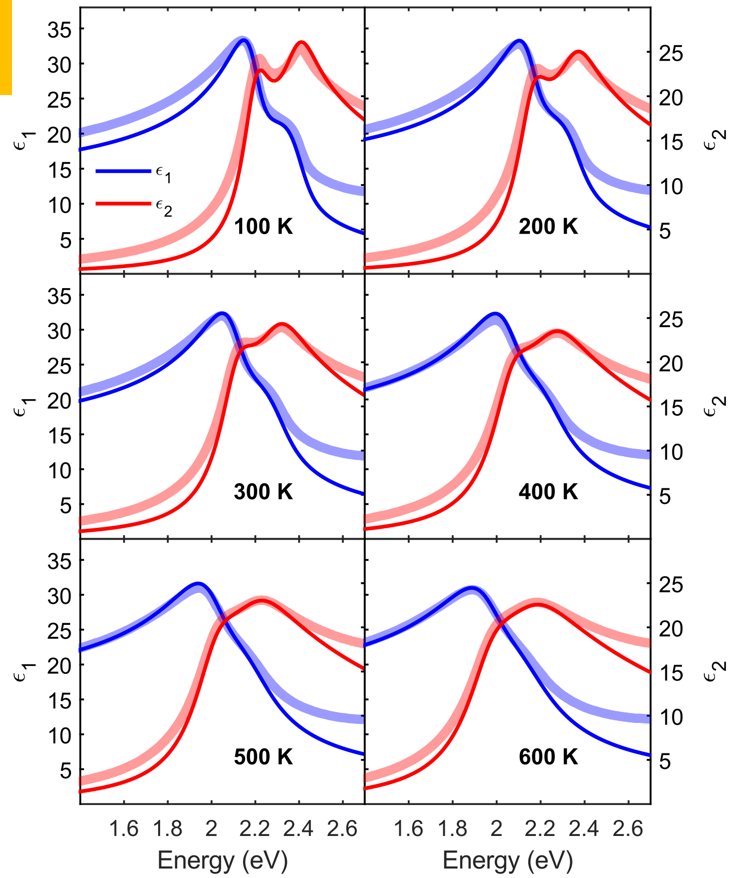

Mismatch of theory and model could be due to surface effects, $k_{\max}$, or $\mu^{(E_1,E_1+\Delta_1)}$.

C. Emminger *et al.*, J. Vac. Sci. Technol. B **38**, 012202 (2020).
L. Viña *et al.*, Phys. Rev. B 30, 1979 (1984).
N. S. Fernando *et al.*, Appl. Surf. Sci. **421**, 905 (2017).

Dielectric function (fitted mass)

$\mu^{(E_1)}$ is larger than $\mu^{(E_1+\Delta_1)}$!

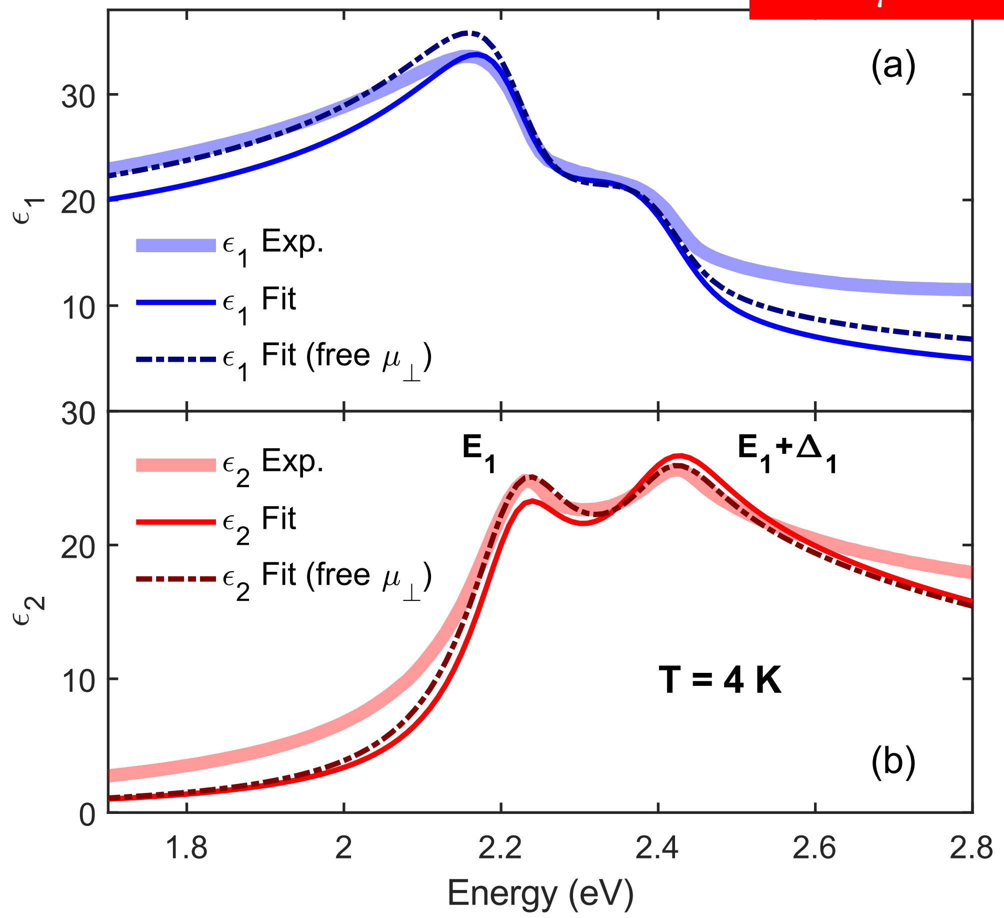

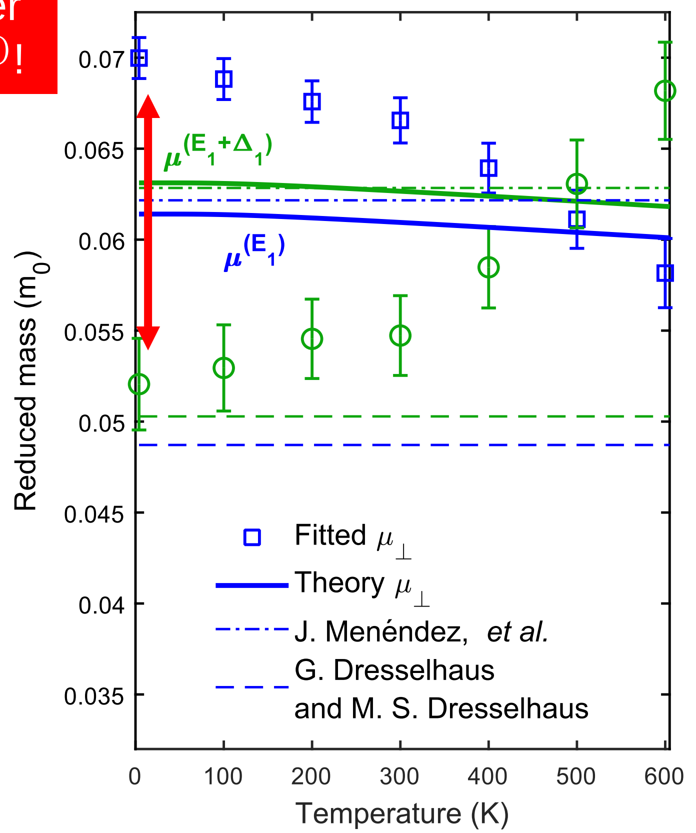

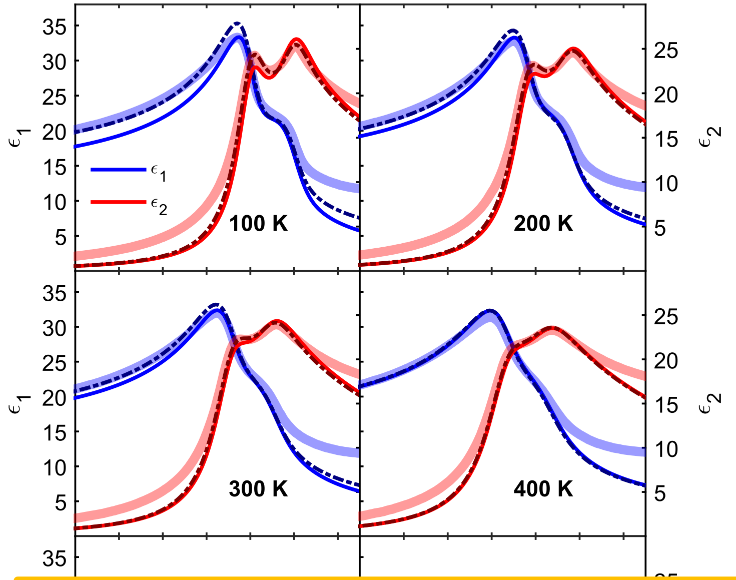

Fit can be improved if $\mu^{(E_1,E_1+\Delta_1)}$ is set as a fitting parameter.

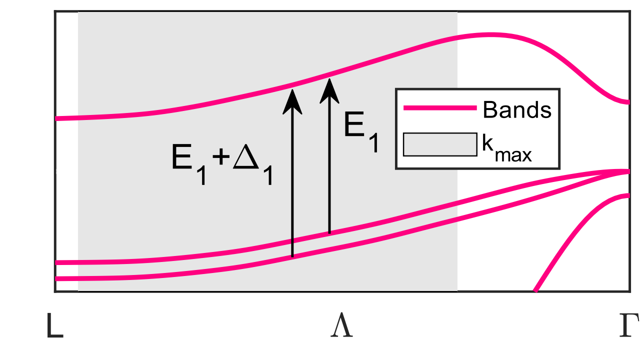

Linear k terms in the bands in the Λ-direction increase $\mu^{(E_1)}$ and decrease $\mu^{(E_1+\Delta_1)}$.

G. Dresselhaus and M. S. Dresselhaus, Phys. Rev. **160**, 649 (1967).
J. Menéndez *et al.*, Phys Rev. B **98**, 165207 (2018).
M. Cardona, Phys. Rev. B **15**,5999 (1977).

Ultrafast measurements

BE BOLD. Shape the Future.®
New Mexico State University

Experimental set-up

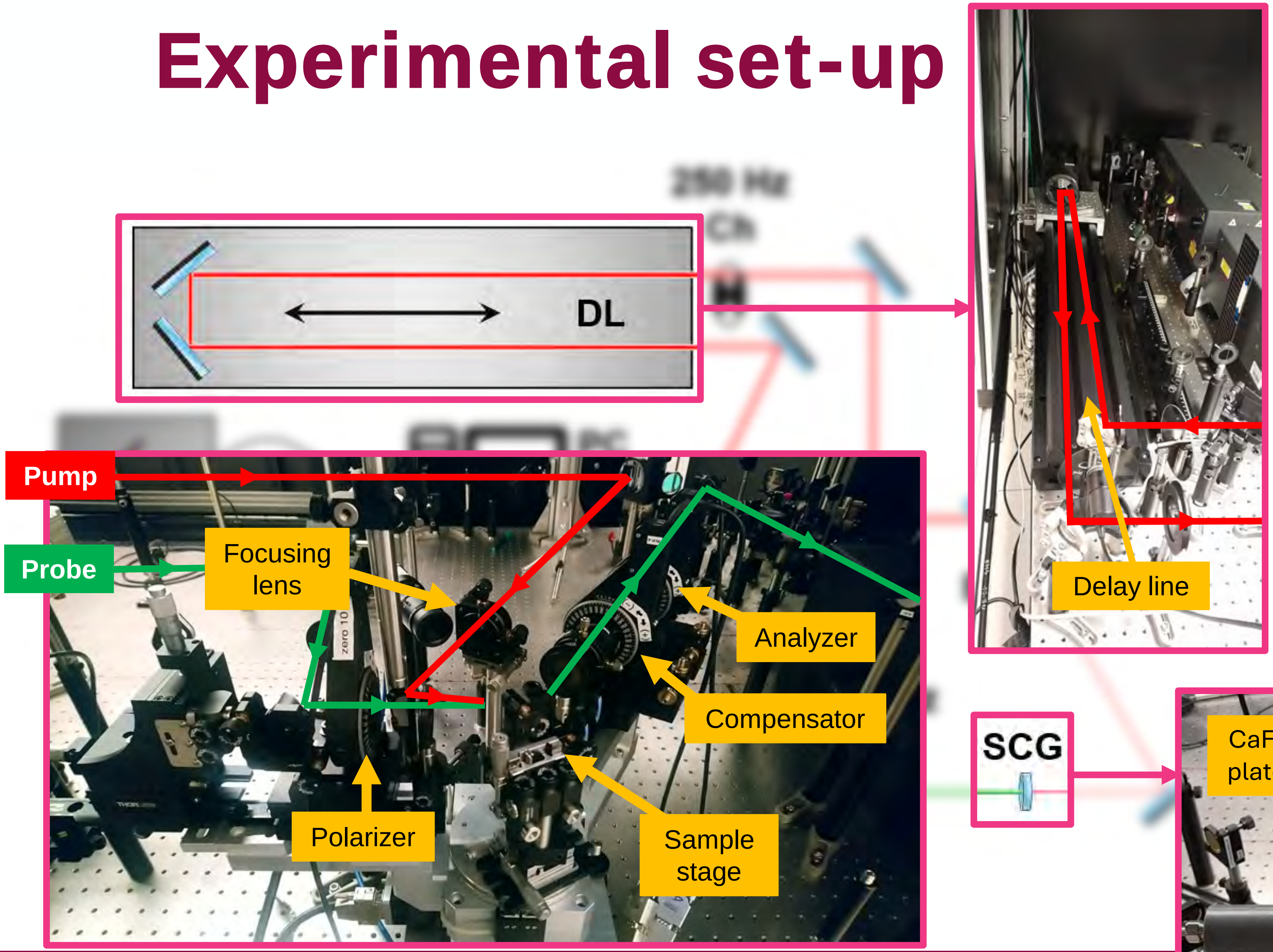

- Ch: Chopper (500 Hz, 250 Hz)
- A: Analyzer
- P: Polarizer
- C_R: Rotating compensator
- L: Lens
- S: Sample
- DL: Delay line (~6.67 ns pump-probe delay and 3 fs resolution)

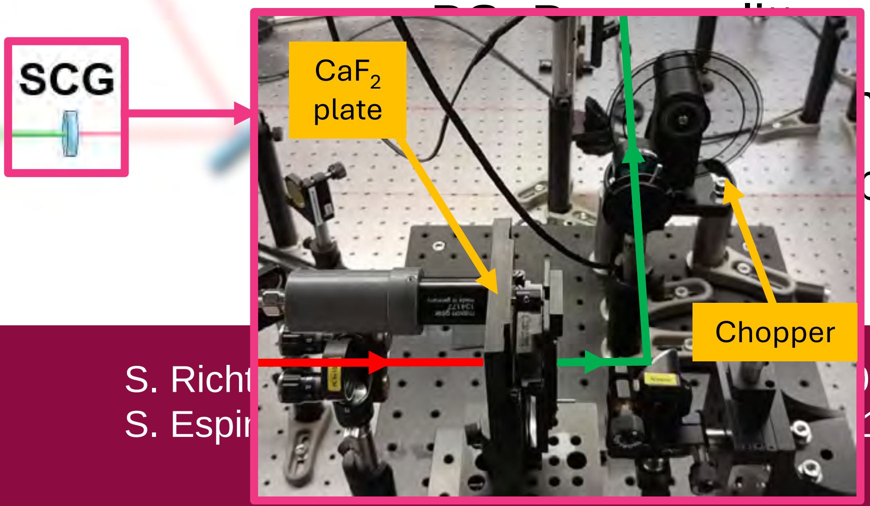

nuum generation

pled device

S. Richt 04 (2021).
S. Espi 105 (2019).

Data reduction

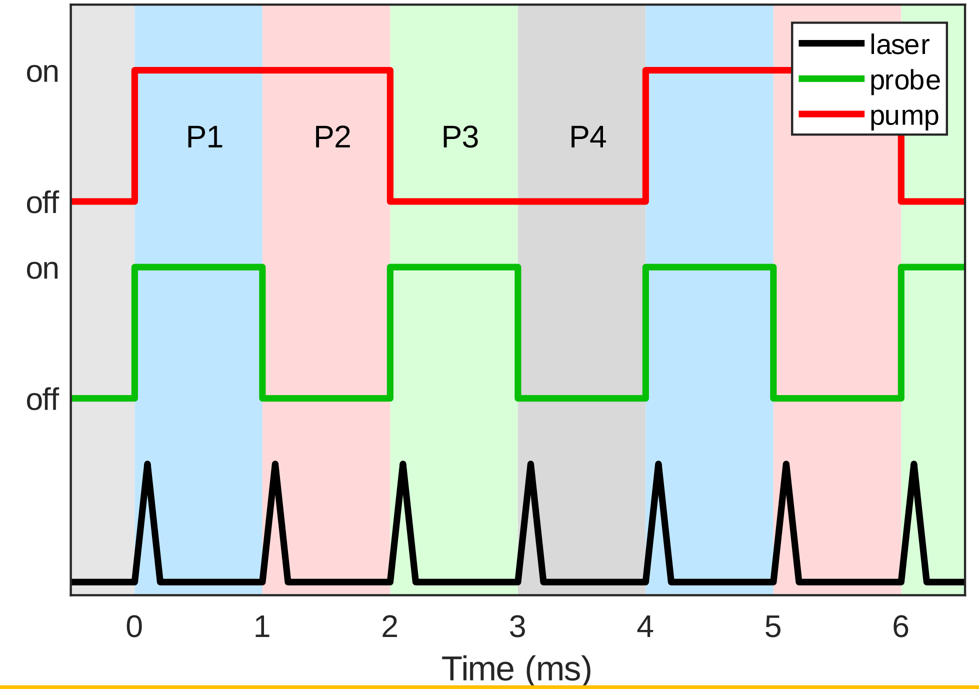

$$\frac{\Delta R^{\mathrm{p}}(E,\Delta t)}{R^{0}(E)} = \frac{I_{\mathrm{P1}} - I_{\mathrm{P2}}}{I_{\mathrm{P3}} - I_{\mathrm{P4}}} - 1$$

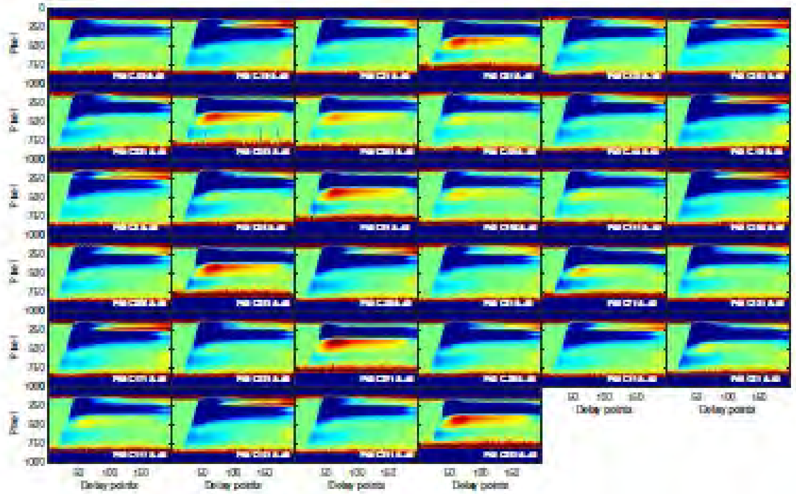

Intensity using reference measurement:

$$I(E,\Delta t) = I^{0}(E)\left[1 + \frac{\Delta R^{\mathrm{p}}(E,\Delta t)}{R^{0}(E)}\right]$$

Moore-Penrose pseudo-inversion

$$M_S = \begin{bmatrix} 1 & -N & 0 & 0 \\ -N & 1 & 0 & 0 \\ 0 & 0 & C & S \\ 0 & 0 & -S & C \end{bmatrix}$$

Ellpsometric angles

$$\tan 2\Psi = \frac{\sqrt{C^2 + S^2}}{N} \qquad \tan 2\Delta = \frac{S}{C}$$

S. Richter *et al.*, Rev. Sci. Instrum. **92**, 033104 (2021).
S. Espinoza *et al.*, Appl. Phys. Lett. **115**, 052105 (2019).

Dielectric constant as a function of delay time

After removing oxide layer.

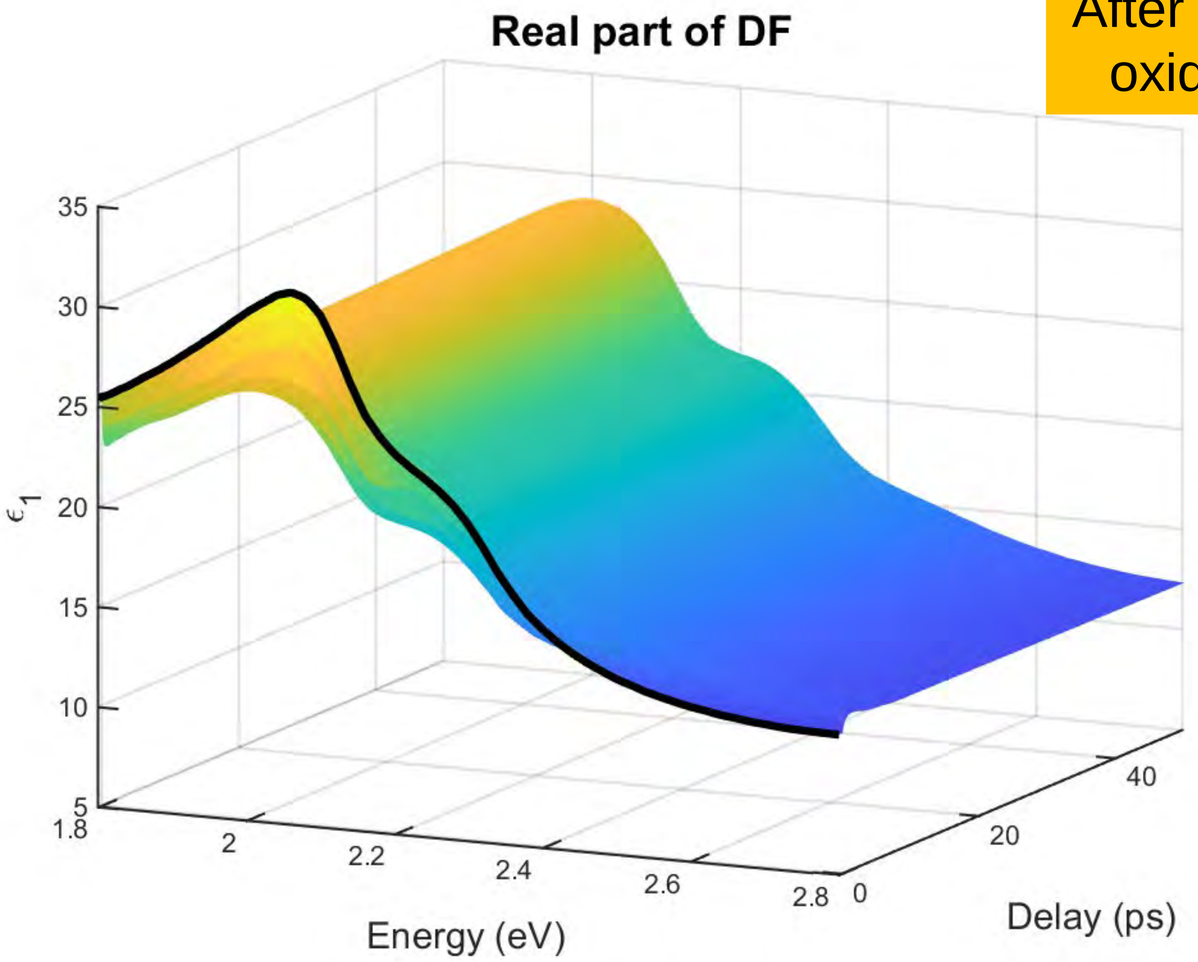

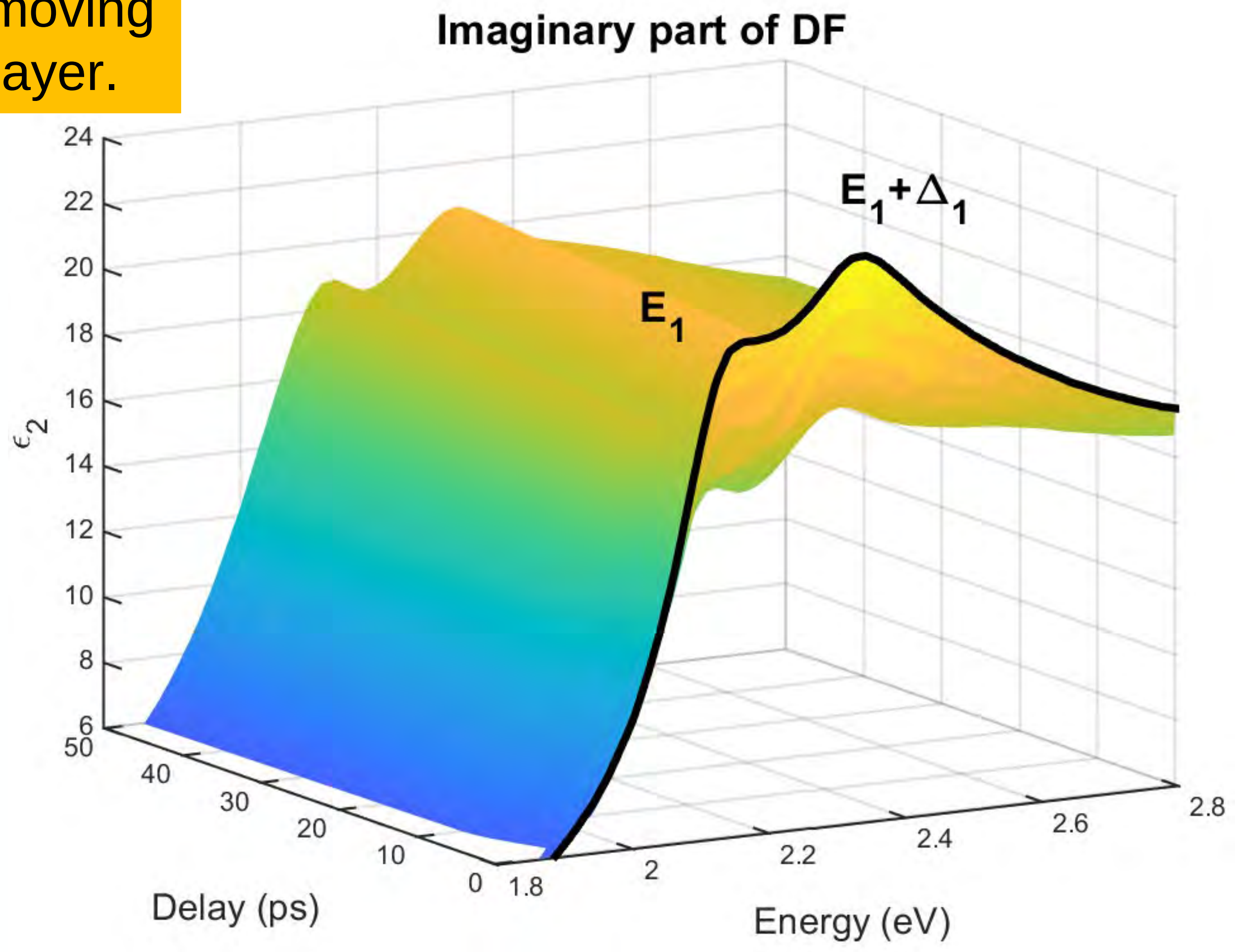

Dielectric constant as a function of delay time

ε almost fully recovers after 100 ps.

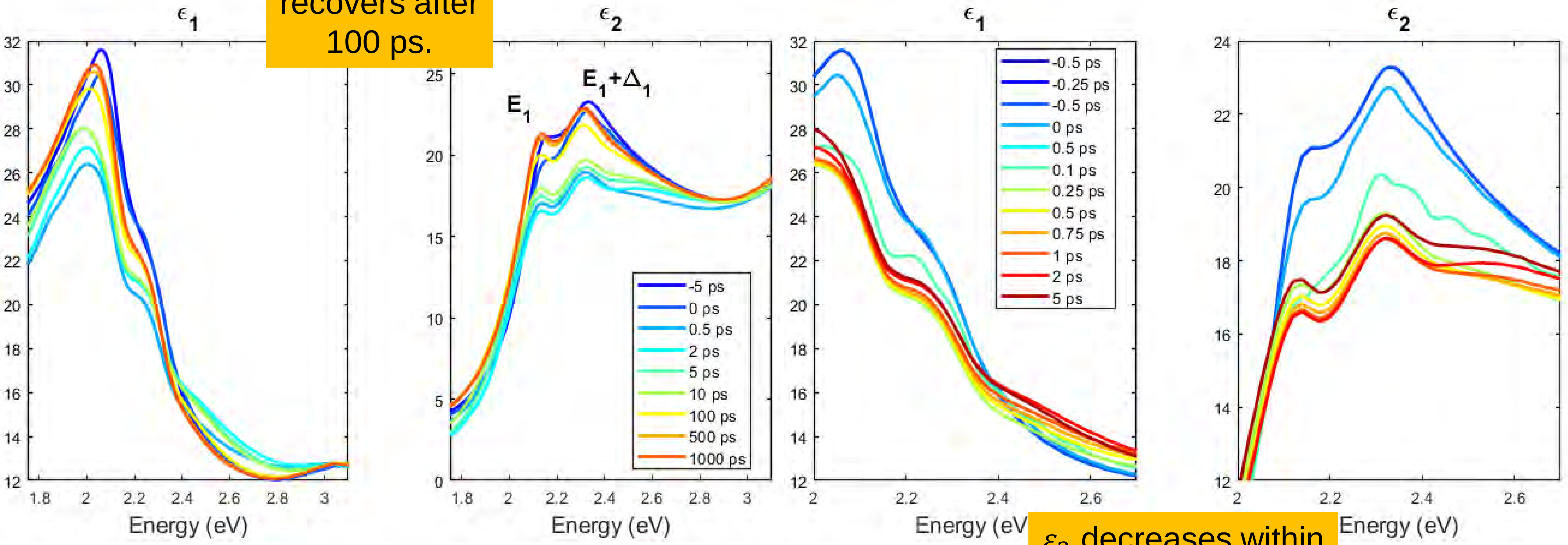

ε_2 decreases within the first ps and recover afterwards.

Carrier statistics

BE BOLD. Shape the Future.®
New Mexico State University

First 100s of femtoseconds

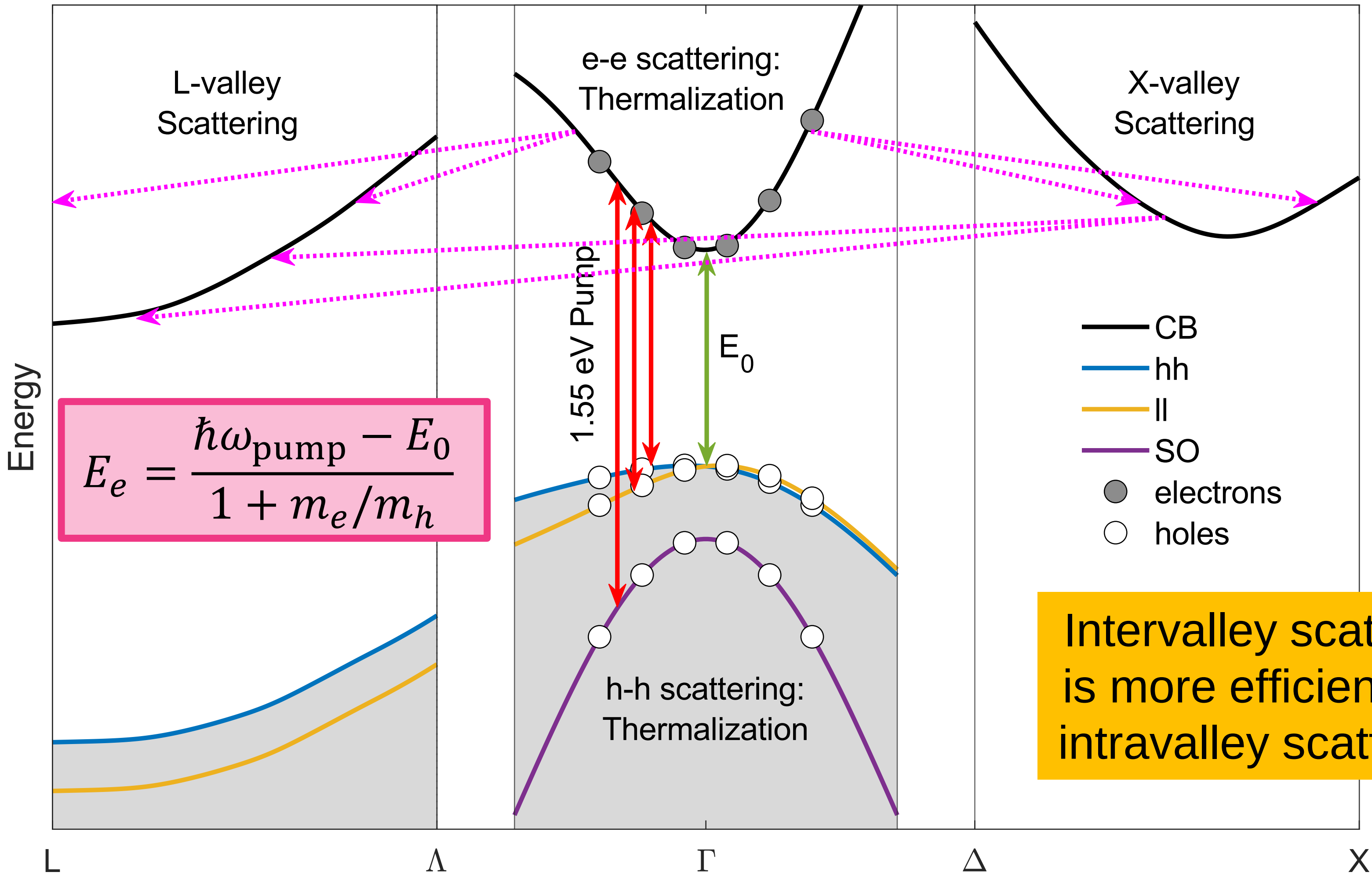

$$E_e = \frac{\hbar\omega_{\text{pump}} - E_0}{1 + m_e/m_h}$$

Intervalley scattering is more efficient than intravalley scattering.

H. Kalt, C. F. Klingshirn, *Semiconductor Optics 2* (Springer, 2024).
R. R. Alfano, *Semiconductors Probed by Ultrafast Laser Spectroscopy I* (Academic Press, 1984).

First picoseconds

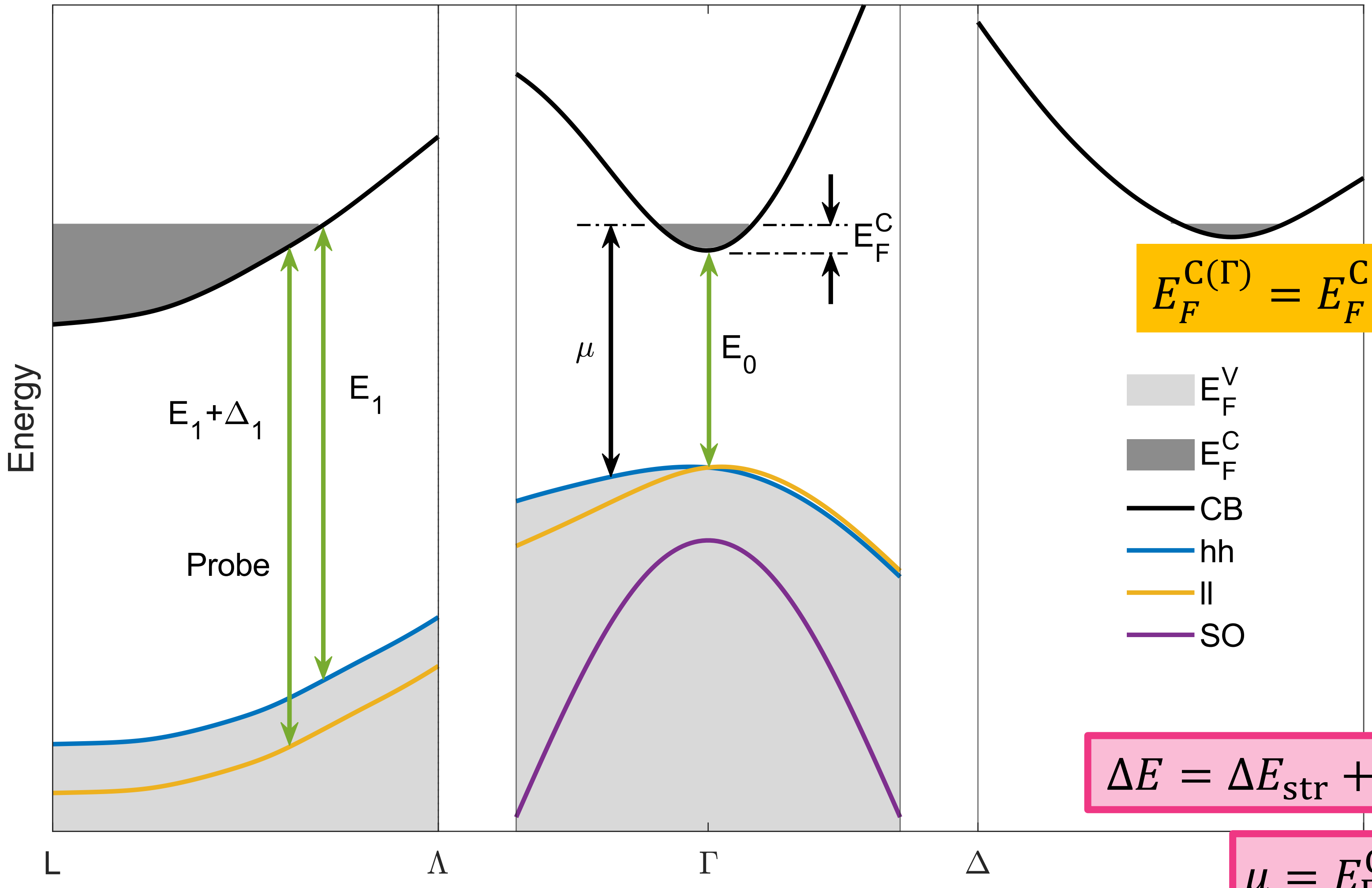

$$E_F^{C(\Gamma)} = E_F^{C(L)} = E_F^{C(X)}$$

$$\Delta E = \Delta E_{\mathrm{str}} + \Delta E_{\mathrm{BGR}} + \Delta E_{\mathrm{BM}}$$

$$\mu = E_{\mathrm{F}}^{\mathrm{C}} + E_g$$

H. Kalt, C. F. Klingshirn, *Semiconductor Optics 2* (Springer, 2024).
P. Vashishta, Appl. Phys. Rev. B. **25**, 6492 (1982).

Charge carrier concentration

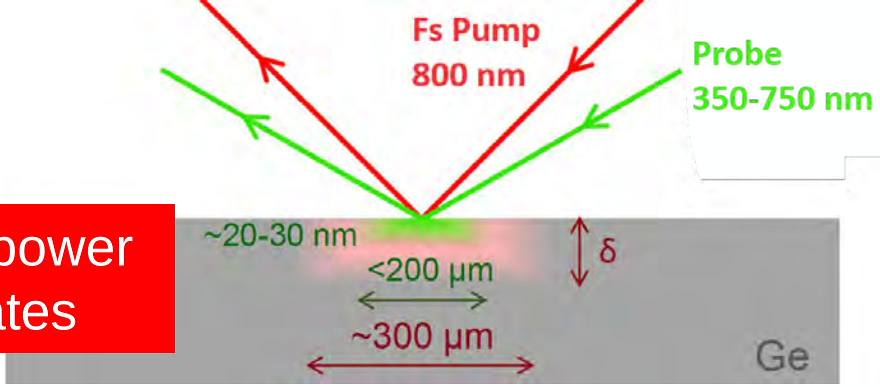

Using pump power overestimates

Plasma temperature:

$$T_c \approx \frac{E_e}{3k_B}$$

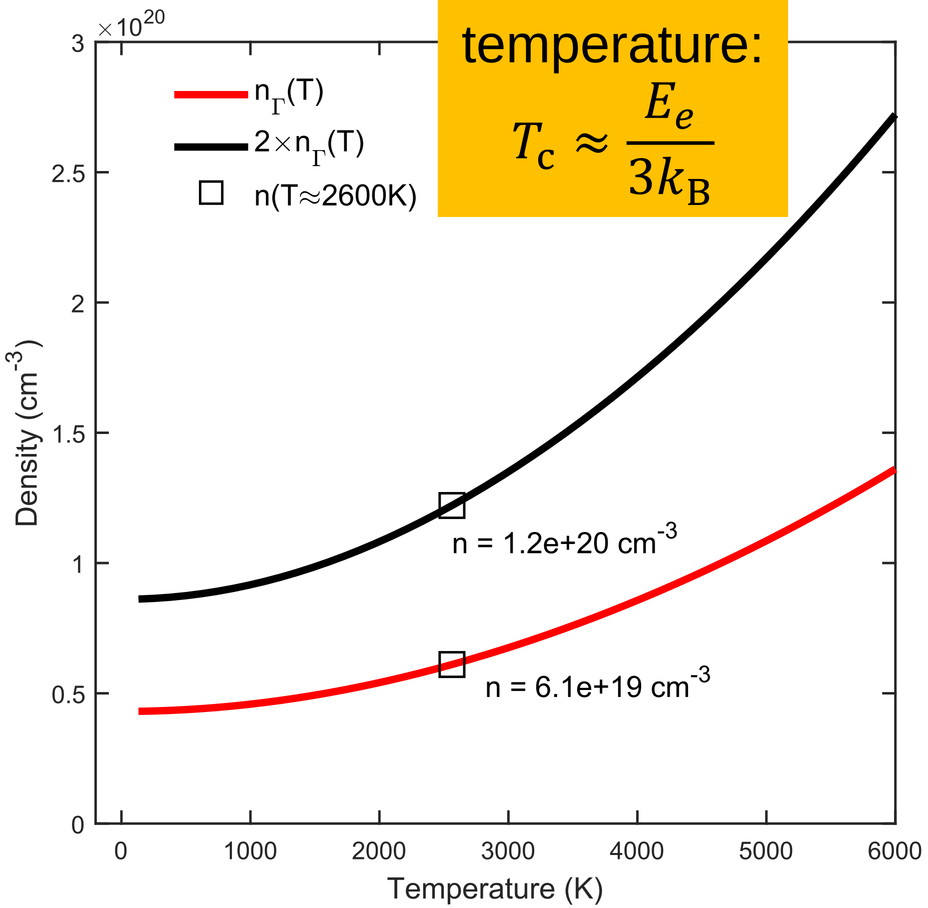

Pump energy imposing the limit to the Fermi energy :

$$n_\Gamma(T) = \frac{1}{4}\left(\frac{2m_{e,\Gamma}k_B T}{\pi\hbar^2}\right)^{3/2} F_{1/2}\left(\frac{E_e}{k_B T}\right) + \mathrm{N.P.},$$

Where N.P. stands for non-parabolicity. On the timescales of the pump-pulse, the carrier density is limited at the Γ-valley.

A. L. Smirl, in *Physics of Nonlinear Transport in Semiconductors*, edited by Kerry, Barker, and Jacoboni (Plenum Press, 1980).
J. Menéndez *et al.*, Phys. Rev. B. **101**, 195204 (2020).

Charge carrier concentration

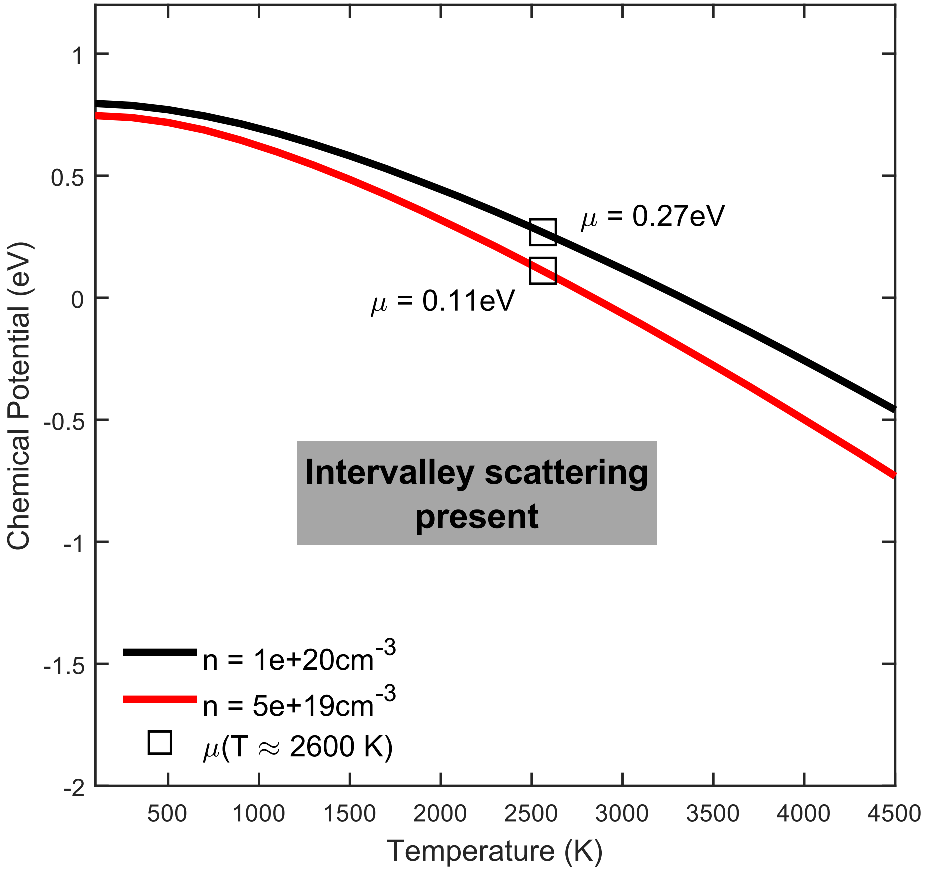

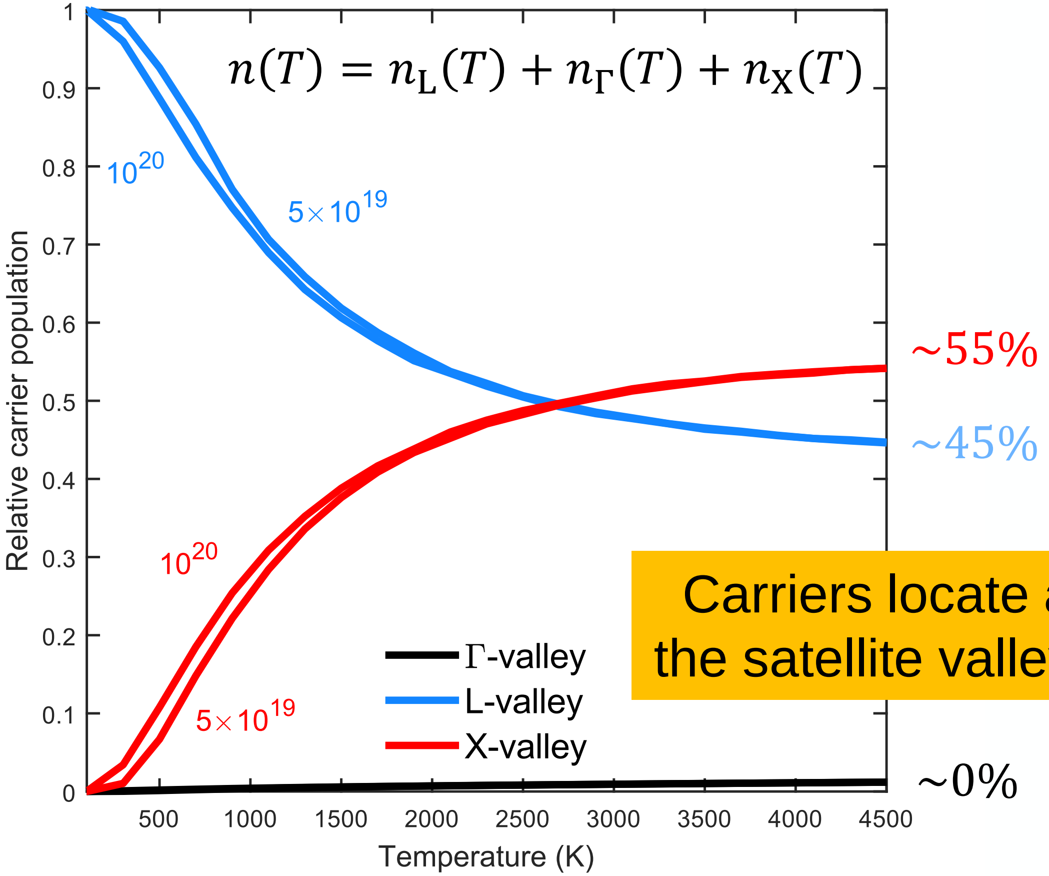

A. L. Smirl, in *Physics of Nonlinear Transport in Semiconductors*, edited by Kerry, Barker, and Jacoboni (Plenum Press, 1980).
J. Menéndez *et al.*, Phys. Rev. B. **101**, 195204 (2020).

Dielectric function model

BE BOLD. Shape the Future.®
New Mexico State University

2D Exciton model

$$g_a(\xi) = 2\ln\xi - 2\psi(1/2 - \xi)$$

$$\varepsilon(E) = \frac{4k_{\max}e^2\bar{P}^2\mu_\perp^{(E_1)}}{3\varepsilon_0 m^2\pi^2(E+i\Gamma)^2}\left\{g_a\left[\sqrt{\frac{R}{E_g-(E+i\Gamma)}}\right]+g_a\left[\sqrt{\frac{R}{E_g-(-E-i\Gamma)}}\right]-2g_a\left[\sqrt{\frac{R}{E_g-(0)}}\right]\right\}$$

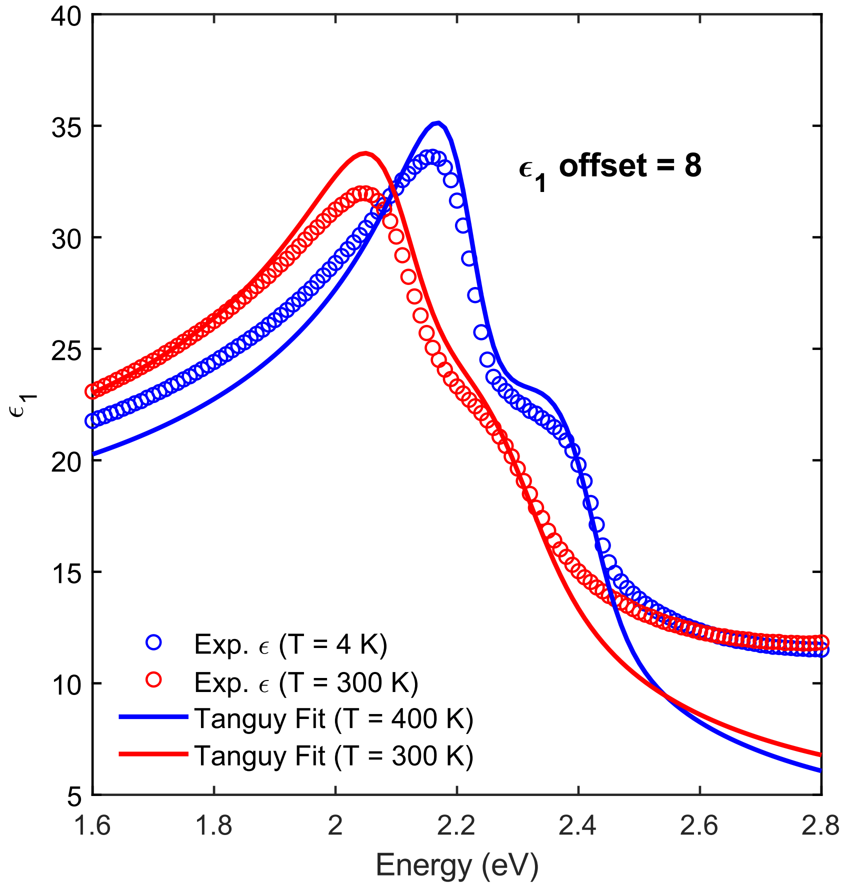

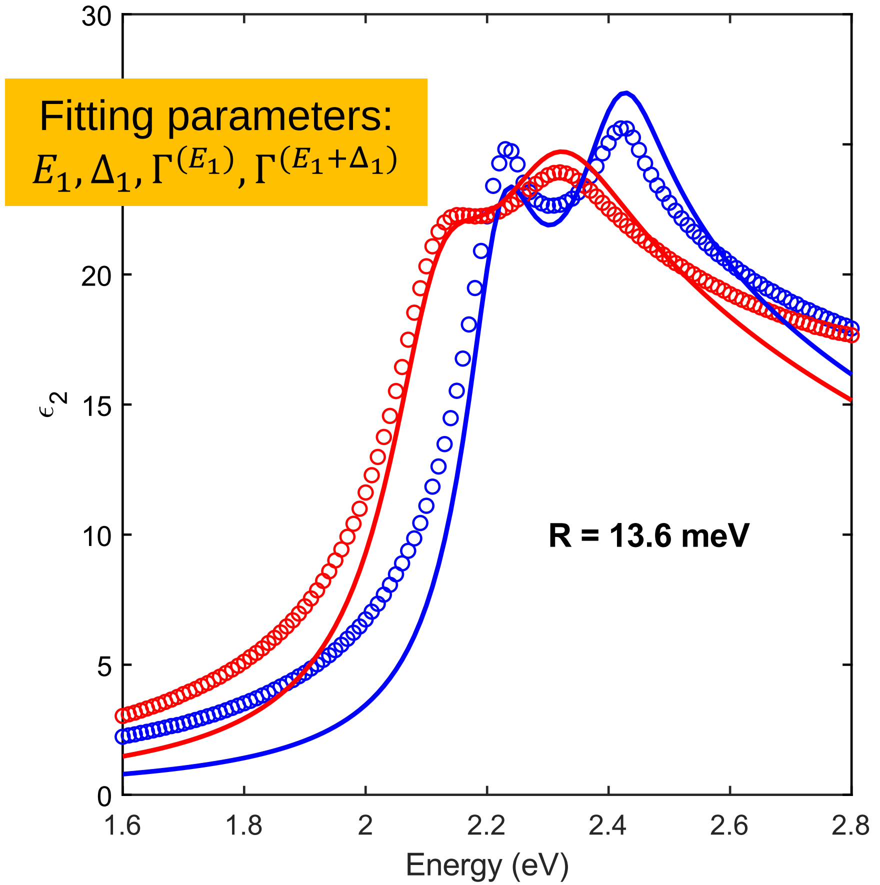

$$k_{\max} = 0.7\frac{\pi\sqrt{3}}{a_0}$$

NM STATE BE BOLD. Shape the Future.®

C. Tanguy, Solid State Commun. **98**, 65 (1996).
C. Emminger *et al.*, J. Vac. Sci. Technol. B **38**, 012202 (2020).
C. A. Armenta and S. Zollner, J. Appl. Phys. **137**, 245101 (2025).

Band-filling model

Fermi singularity is more prominent as temperature decreases.

$$\varepsilon_2(E) = \frac{2e^2\bar{P}^2\mu_\perp}{3\varepsilon_0\pi^2 m^2 E^2} H(E-E_1) \int_{-k_{\max}}^{k_{\max}} 1 - f[E_c(E,k_z^2)]dk_z$$

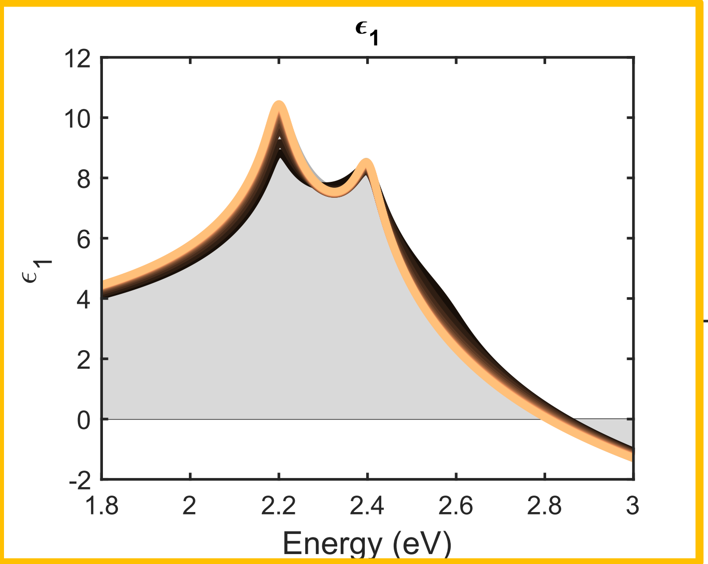

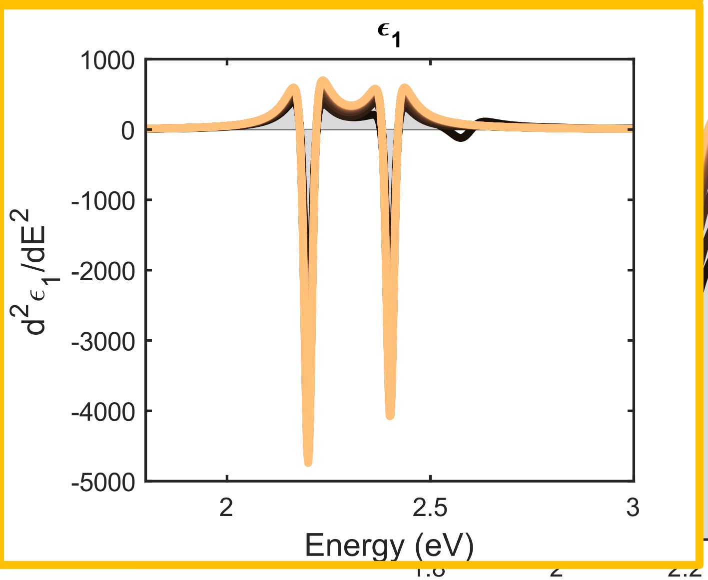

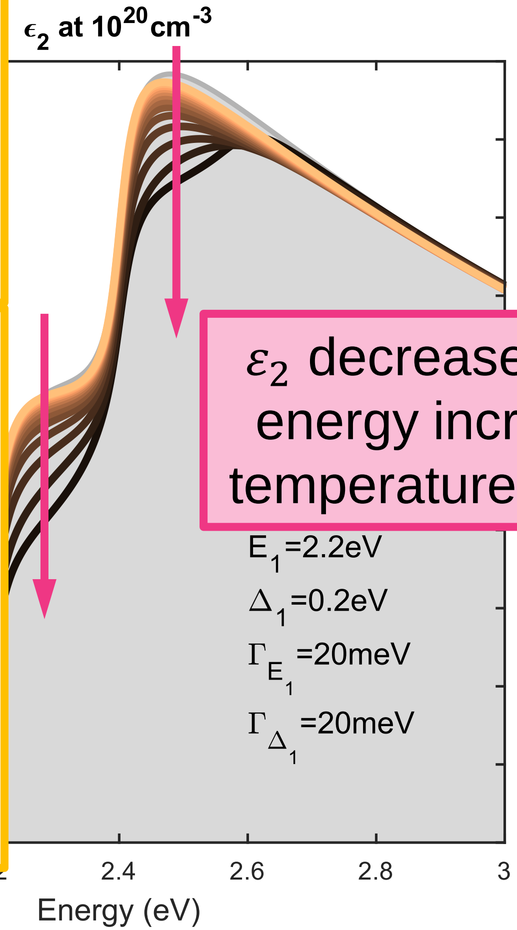

ε_2 decreases as Fermi energy increases and temperature decreases.

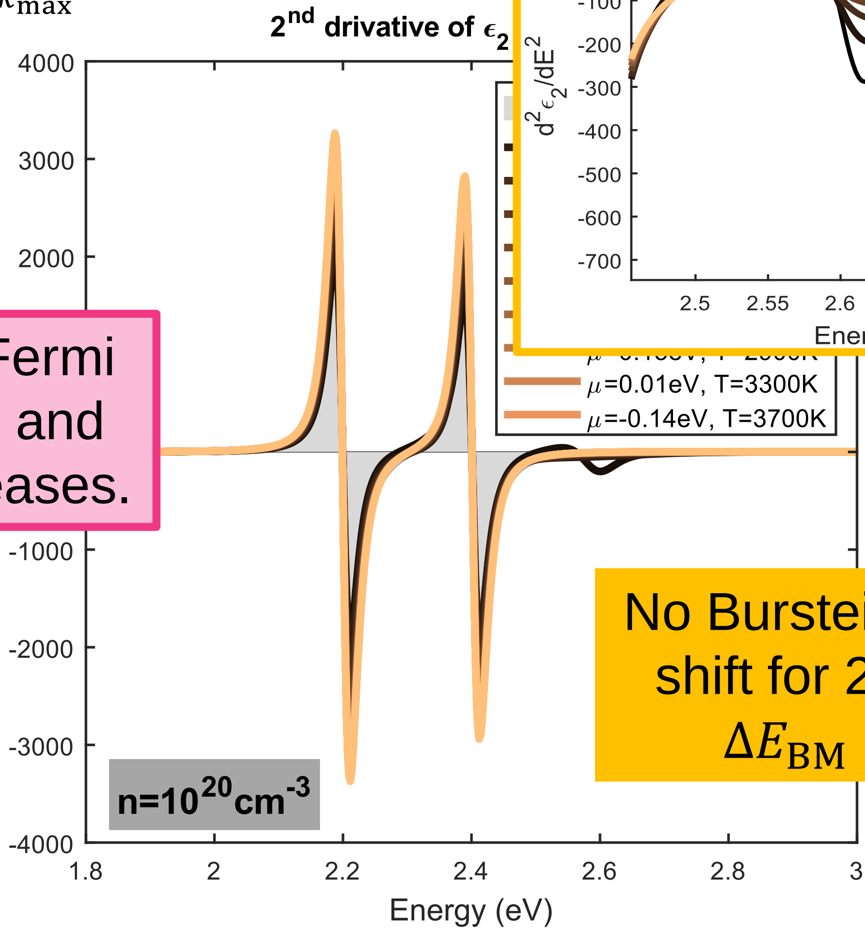

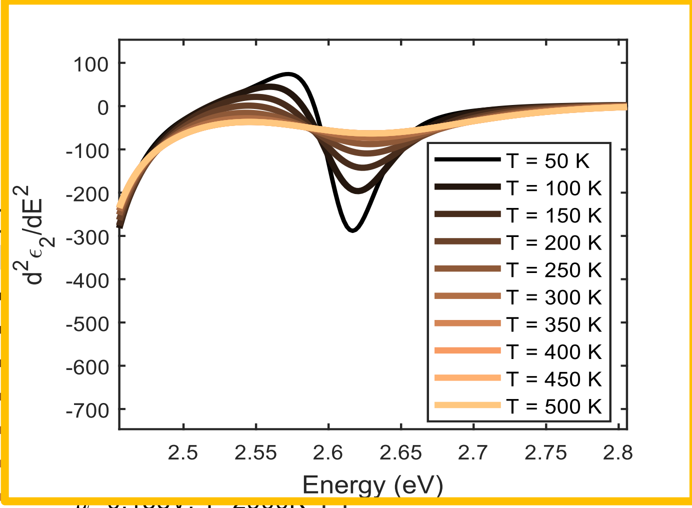

No Burstein-Moss shift for 2D CP:
$\Delta E_{\mathrm{BM}} = 0$

C. Xu *et al.*, J. Appl. Phys. **125**, 085704 (2019).
C. Xu *et al.*, Phys. Rev. Lett. **118**, 267402 (2017).

Fitted data

BE BOLD. Shape the Future.®
New Mexico State University

Final model

2D exciton model with band filling effects:

$$\varepsilon_2(E) = \frac{2e^2\mu_\perp^{(E_g)}\bar{P}^2}{3\varepsilon_0 m^2\pi}\,\mathrm{Im}\left\{\frac{g_a[\xi(E+i\Gamma)]+g_a[\xi(-E-i\Gamma)]-2g_a[\xi(0)]}{(E+i\Gamma)^2}\right\}\int_{-k_{\max}}^{k_{\max}}\{1-f[E_c(E,k_z^2)]\}dk_z$$

Negative delays (steady state)

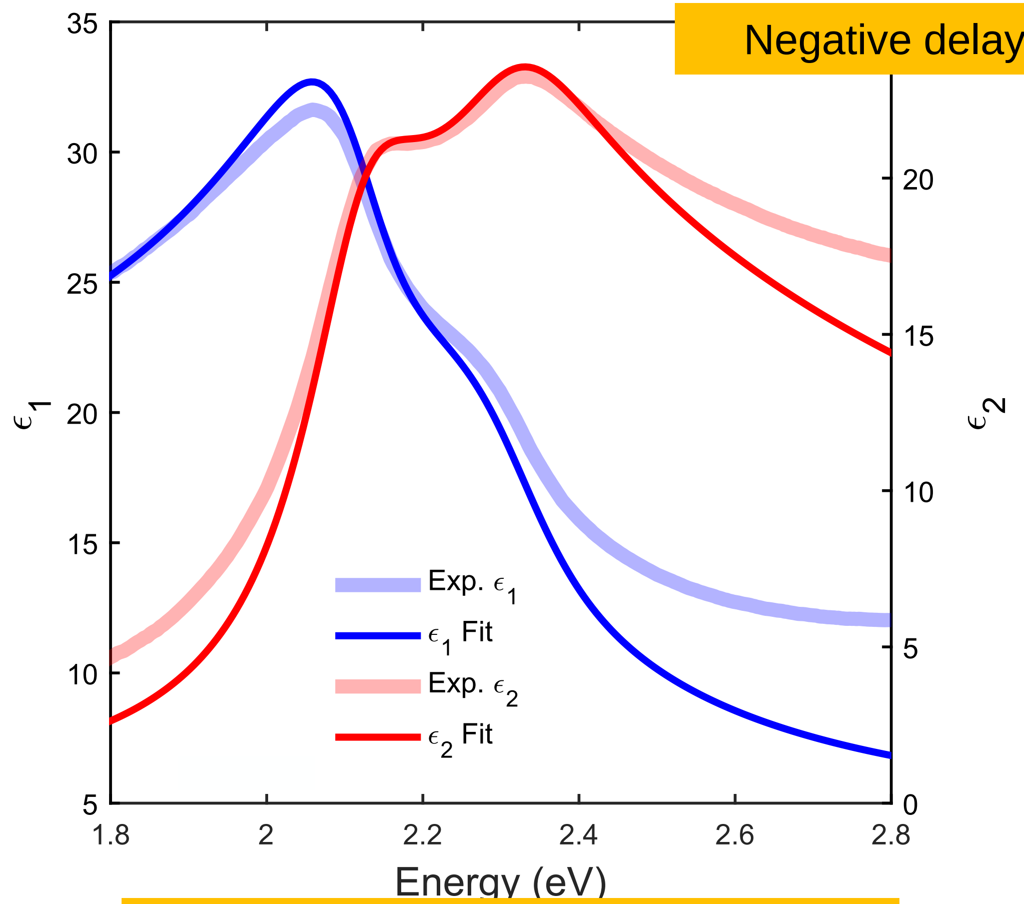

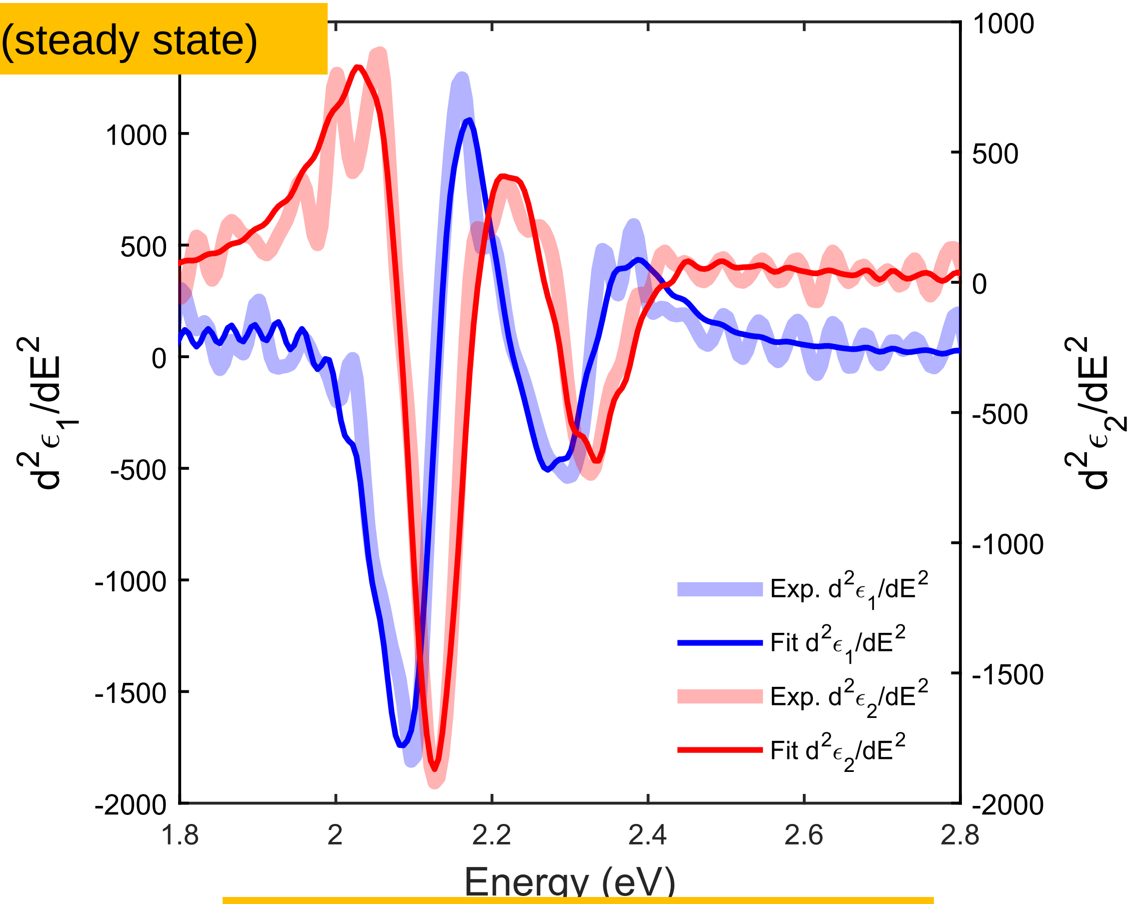

Dielectric function fitting parameters:
$\mu^{(E_1)}, \mu^{(E_1+\Delta_1)}$

2nd derivative itting parameters:
$E_1, \Delta_1, \Gamma^{(E_1)}, \Gamma^{(E_1+\Delta_1)}$
Parameters T_c and n are at thermal equilibrium.

NM STATE BE BOLD. Shape the Future.®

Final model

2D exciton model with band filling effects:

$$\varepsilon_2(E) = \frac{2e^2\mu_\perp^{(E_g)}\bar{P}^2}{3\varepsilon_0 m^2\pi}\,\mathrm{Im}\left\{\frac{g_a[\xi(E+i\Gamma)] + g_a[\xi(-E-i\Gamma)] - 2g_a[\xi(0)]}{(E+i\Gamma)^2}\right\}\int_{-k_{\max}}^{k_{\max}}\{1 - f[E_c(E,k_z^2)]\}dk_z$$

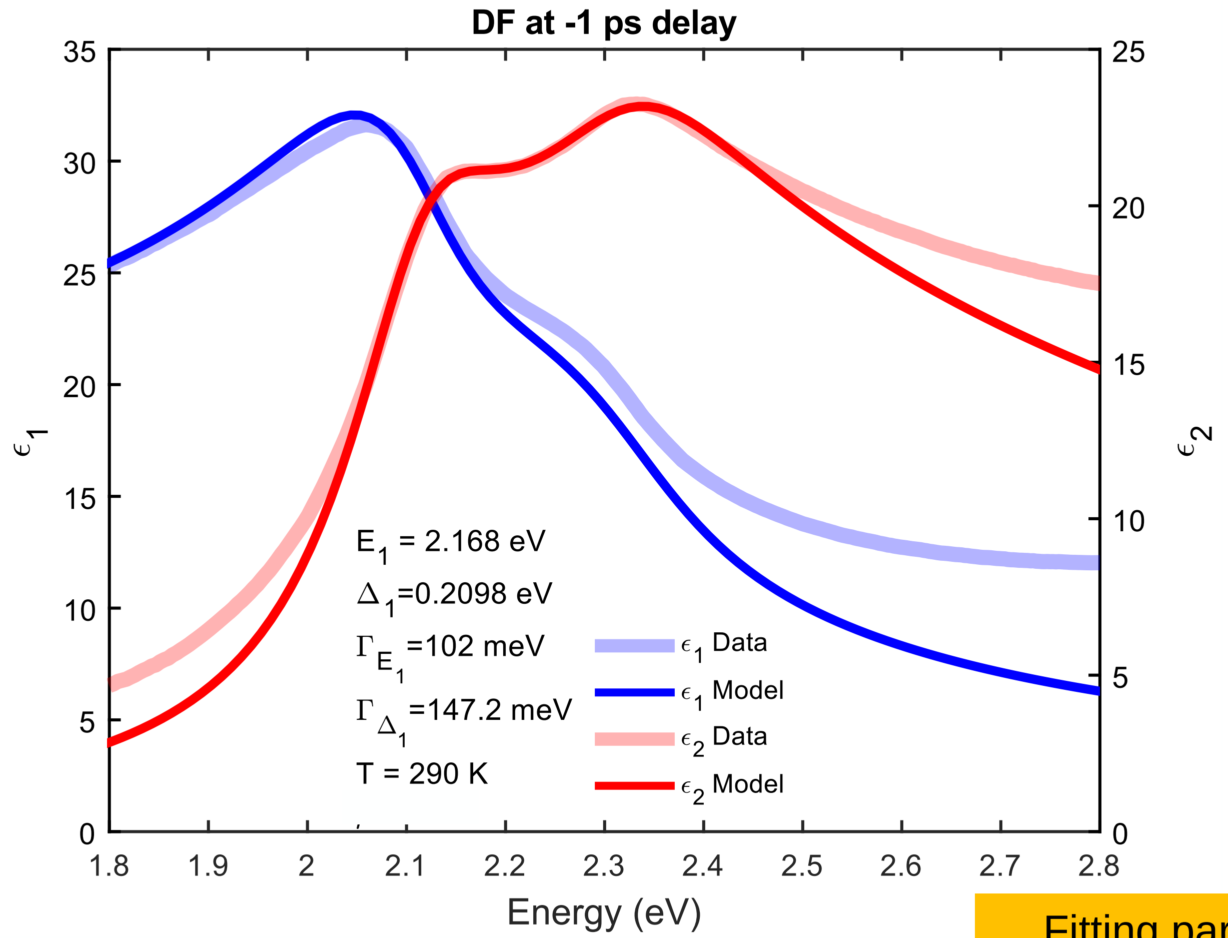

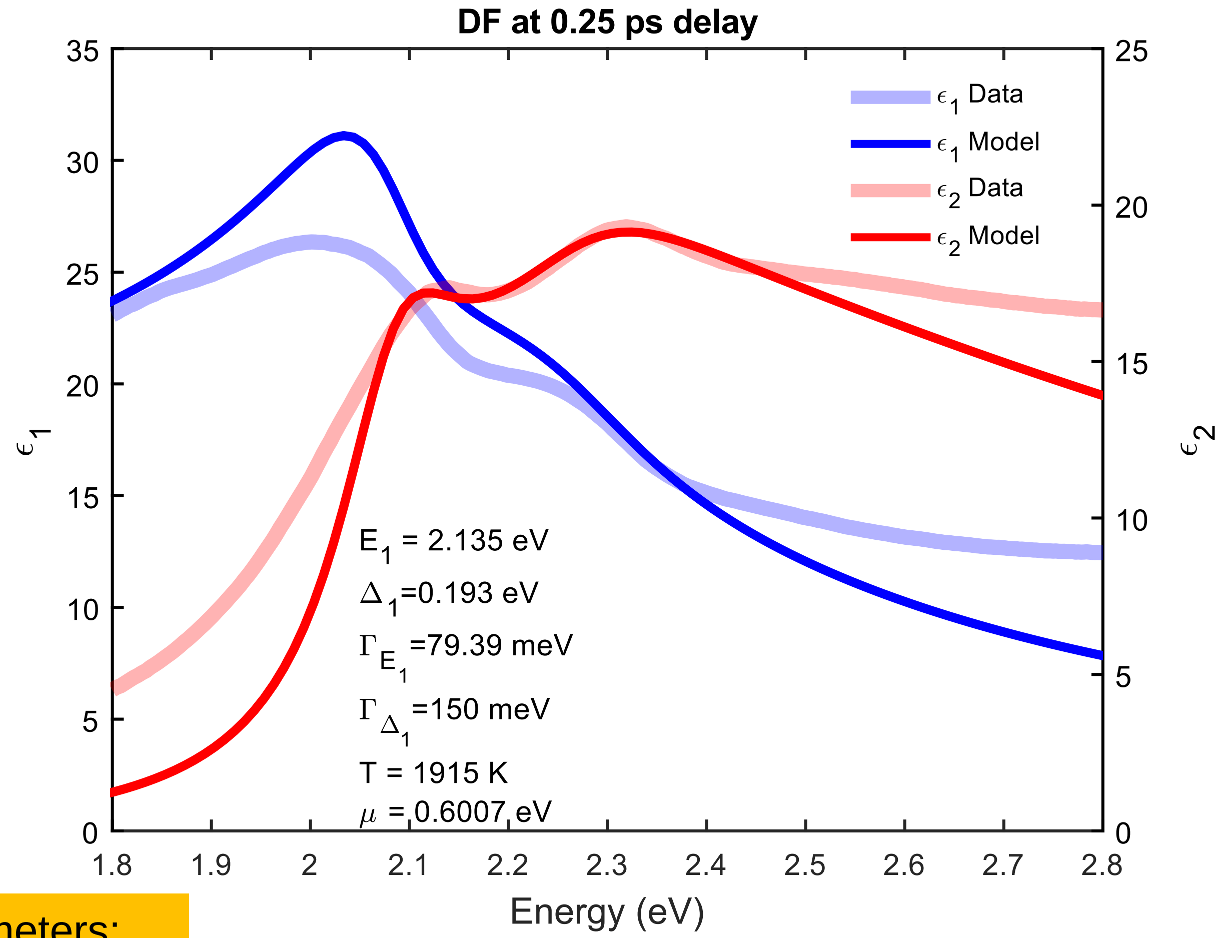

Fitting parameters:
$E_1, \Delta_1, \Gamma^{(E_1)}, \Gamma^{(E_1+\Delta_1)}, T_c, n$

NM STATE BE BOLD. Shape the Future.®

Final model

2D exciton model with band filling effects:

$$\varepsilon_2(E) = \frac{2e^2\mu_\perp^{(E_g)}\bar{P}^2}{3\varepsilon_0 m^2 \pi}\,\mathrm{Im}\left\{\frac{g_a[\xi(E+i\Gamma)] + g_a[\xi(-E-i\Gamma)] - 2g_a[\xi(0)]}{(E+i\Gamma)^2}\right\}\int^{k_{max}}\{1 - f[E_c(E,k_z^2)]\}dk_z$$

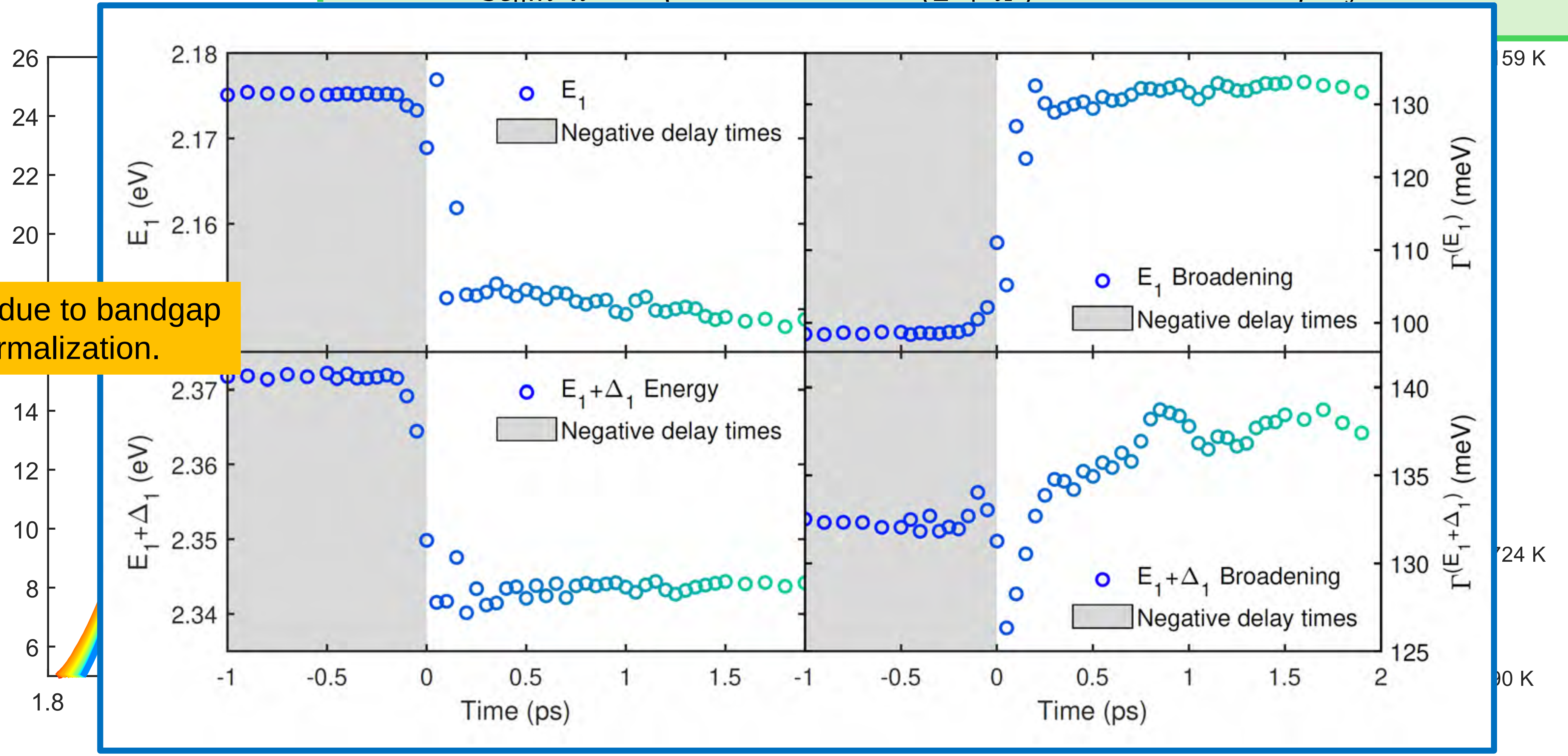

Redshift due to bandgap renormalization.

L. Viña and M. Cardona, Phys. Rev. B **29**, 6739 (1984).

Carrier relaxation

Phonons emitted every 4 to 18 fs, compared to the literature value of ~50 fs.

We approximated the overall energy relaxation to

$$\left\langle \frac{\mathrm{d}E}{\mathrm{d}t} \right\rangle = \frac{Ae^{-\frac{t}{\tau}}}{\tau}$$

At its highest relaxation rate, energy is being dissipated by emitting a phonon around every 4 to 18 femtoseconds.

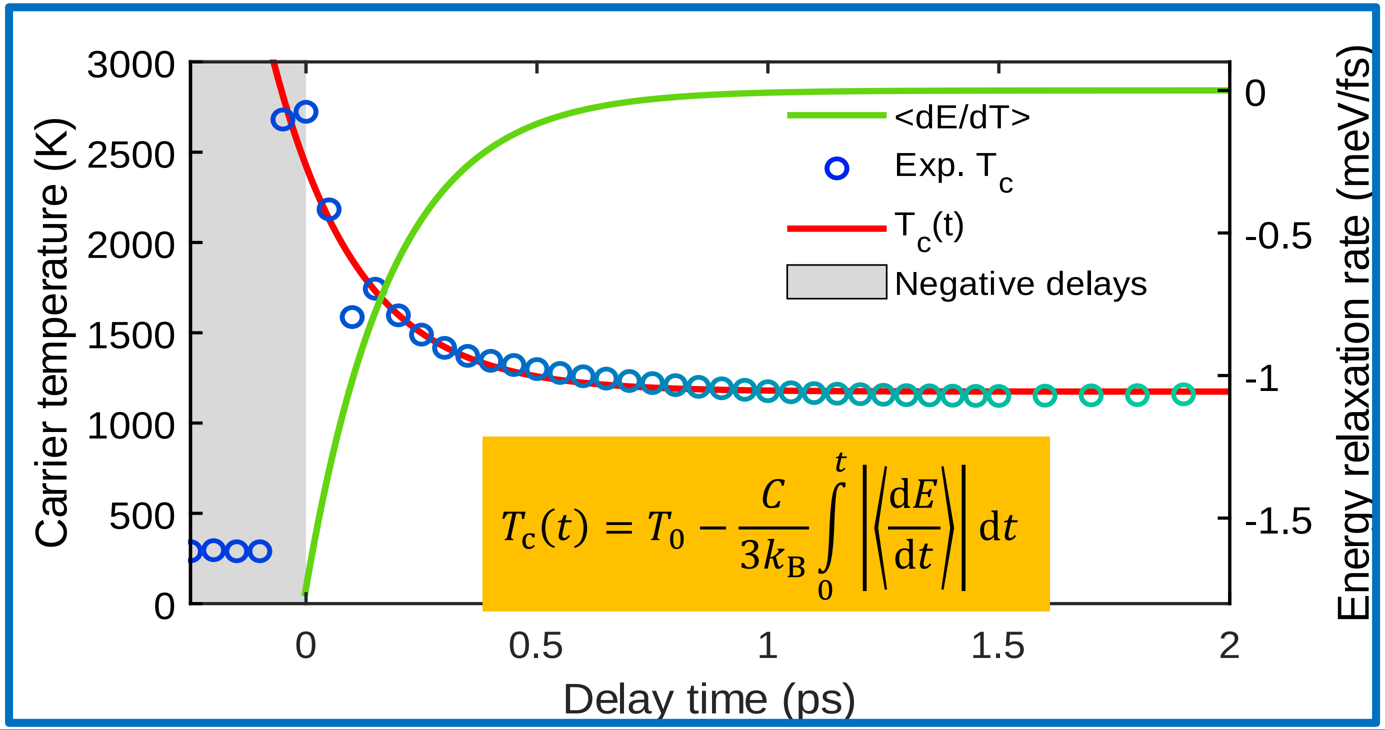

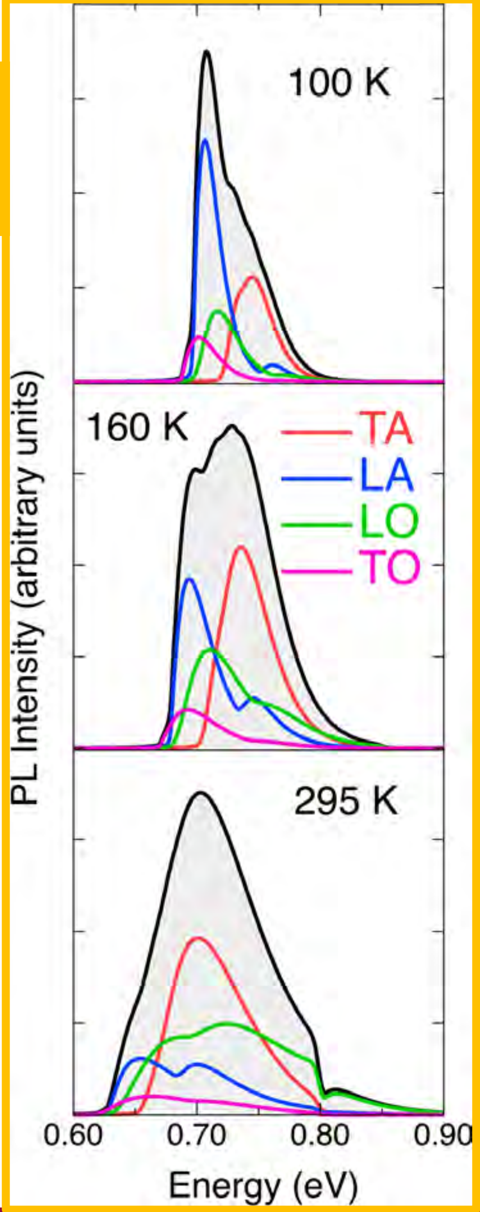

J. Shah and R. F. Leheny, in *Semiconductors Probed by Ultrafast Laser Spectroscopy Volume I*, edited by R. R. Alfano (Academic Press, 1984).
J. Menéndez *et al.*, Phys. Rev. B **101**, 195204 (2020).
S. Zollner *et al.*, Solid State Commun. **76**, 877 (1990).

Modeling additional processes

BE BOLD. Shape the Future.®
New Mexico State University

Free carrier absorption and excitonic screening

Additional absorption processes:

- Free carrier absorption (Drude model):

$$\varepsilon\,(E) = \varepsilon_{\mathrm{st}}\left(1 - \frac{\omega_{\mathrm{p}}^2}{\omega^2 + i\Gamma\omega}\right)$$

- Excitonic screening: Coulomb interaction between carrier in the exciton system is screened by the presence of additional carriers.

$$\varepsilon^{3\mathrm{D}}(E) = \frac{A\sqrt{R}}{(E + i\Gamma)^2}\{\tilde{g}[\xi(E + i\Gamma)] + \tilde{g}[\xi(-E - i\Gamma)] - 2\tilde{g}[\xi(0)]\}$$

$$\xi(z) = \frac{2}{\sqrt{\frac{E_g - z}{R}} + \sqrt{\frac{E_g - z}{R} + \frac{4}{g}}}$$

Currently, no solution for excitonic screening in 2D exists.

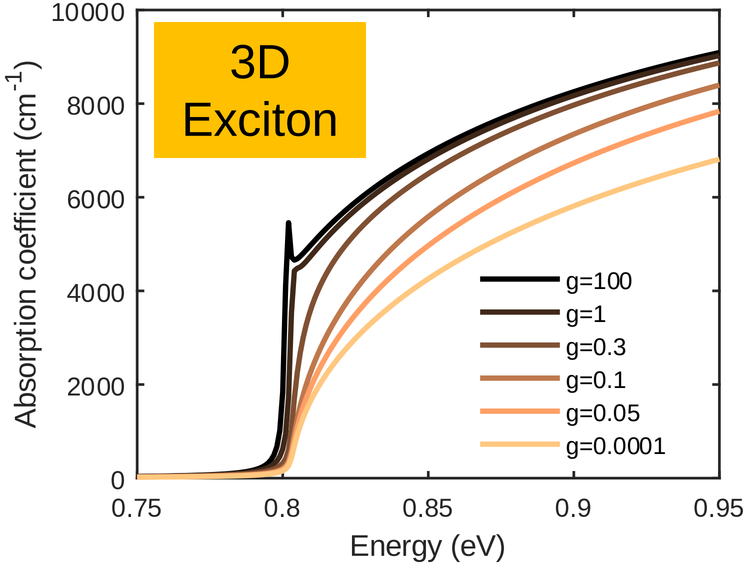

C. Tanguy, Phys. Rev. B **60**, 10660 (1999).

Conclusion and future work

- Significant changes in the dielectric function of bulk Ge were observed. We primarily focus on the decrease in amplitude of ε_2 within the first ps.
- Carrier statistics provide the photoexcited carrier density, as well as the initial and evolution of the parameters of our model.
- Band filling plus 2D exciton model looks reasonable when compared with the experimental dielectric function.
- Bandgap renormalization is smaller than expected due to the only considering many-body effetcs. Carrier relaxation shows the emission of phonon every 4 to 18 fs.
- The model neglects
  - Diffusion of carriers
  - **<u>Excitonic screening</u>**
  - Laser induced strain, local heating

Thank you!

QUESTIONS?

BE BOLD. Shape the Future.®
New Mexico State University

E_1 and $E_1+\Delta_1$ critical points

Use $\vec{k}\cdot\vec{p}$ theory and Bloch's theorem:

$$\left(\underbrace{\frac{p^2}{2m_0}+V}_{H_0}+\underbrace{\frac{\hbar\vec{k}\cdot\vec{p}}{m_0}}_{H_{\vec{k}}}+\frac{\hbar^2k^2}{2m_0}\right)u_{n\vec{k}}=E_{n\vec{k}}u_{n\vec{k}}$$

Only similar spins will couple. If the only non-zero elements are

$$\bar{P}=-i\langle Z|p_x|X\rangle=-i\langle Z|p_y|Y\rangle,$$

Then the Hamiltonian diagonalizes as:

$$0=\det\left(H_0+H_{\vec{k}}-\tilde{E}\right)=\det\begin{vmatrix} E_1-\tilde{E} & \frac{i\hbar\bar{P}}{m_0\sqrt{2}}k_\perp & \frac{i\hbar\bar{P}}{m_0\sqrt{2}}k_\perp \\ -\frac{i\hbar\bar{P}}{m\sqrt{2}}k_\perp & -\tilde{E} & 0 \\ -\frac{i\hbar\bar{P}}{m_0\sqrt{2}}k_\perp & 0 & -\Delta_1-\tilde{E} \end{vmatrix}$$

Where $\tilde{E}=E-\frac{\hbar^2k^2}{2m_0}$. The characteristic equation is

$$\tilde{E}^3-(E_1-\Delta_1)\tilde{E}^2-\left(E_1\Delta_1+\frac{\hbar^2\bar{P}^2}{m_0^2}k_\perp^2\right)\tilde{E}-\frac{\hbar^2\bar{P}^2\Delta_1}{2m_0^2}k_\perp^2=0.$$

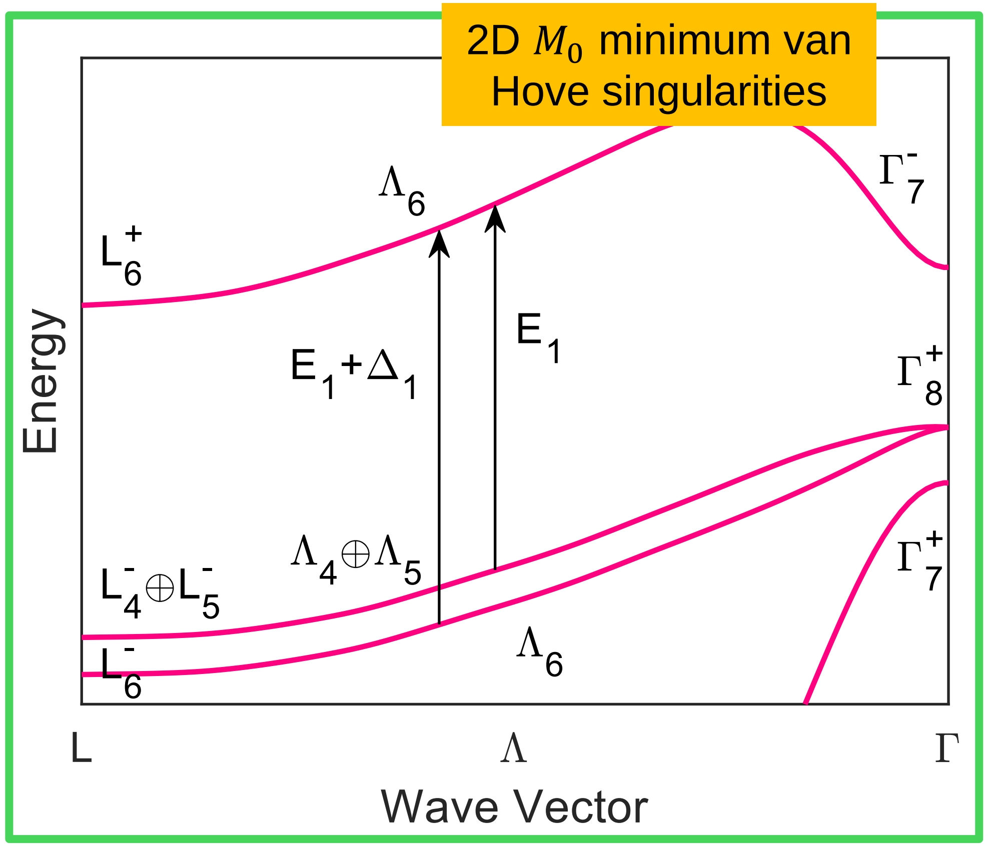

Basis:

$$L_6^+:|Z\uparrow\rangle,|Z\downarrow\rangle$$

$$L_4^-\oplus L_5^-:\frac{1}{\sqrt{2}}|(X+iY)\uparrow\rangle,\frac{1}{\sqrt{2}}|(X-iY)\downarrow\rangle$$

$$L_6^-:\frac{1}{\sqrt{2}}|(X+iY)\ \downarrow\rangle,\frac{1}{\sqrt{2}}|(X-iY)\uparrow\rangle$$

P. Yu, M. Cardona, *Fundamentals of Semiconductors* (Springer, Berlin, 1996).
E. O. Kane, J. Phys. Chem. Solids **1**, 249 (1957).

Effective masses

For small $k_\perp$ (parabolic approximation),

$$E_{\rm CB}(k_\perp) = E_1 + \frac{\hbar^2 k_\perp^2}{2m_0}\underbrace{\left(1+\frac{\bar{P}^2}{m_0}\left[\frac{1}{E_1}+\frac{1}{E_1+\Delta_1}\right]\right)}_{m_\perp^{(L_6^+)}},$$

$$E_{\rm hh}(k_\perp) = \frac{\hbar^2 k_\perp^2}{2m_0}\underbrace{\left(1-\frac{\bar{P}^2}{m_0 E_1}\right)}_{m_\perp^{(L_4^-\oplus L_5^-)}}, \text{ and } E_{\rm lh}(k_\perp) = -\Delta_1 + \frac{\hbar^2 k_\perp^2}{2m_0}\underbrace{\left(1-\frac{\bar{P}^2}{m_0(E_1+\Delta_1)}\right)}_{m_\perp^{(L_6^-)}}.$$

Reduced masses:

$$\frac{1}{\mu_\perp^{(E_1)}} = \frac{1}{m_\perp^{(L_6^+)}} - \frac{1}{m_\perp^{(L_4^-\oplus L_5^-)}} = \frac{\bar{P}^2}{m_0}\left(\frac{2}{E_1}+\frac{1}{E_1+\Delta_1}\right)$$

$$\frac{1}{\mu_\perp^{(E_1+\Delta_1)}} = \frac{1}{m_\perp^{(L_6^+)}} - \frac{1}{m_\perp^{(L_6^-)}} = \frac{\bar{P}^2}{m_0}\left(\frac{1}{E_1}+\frac{2}{E_1+\Delta_1}\right)$$

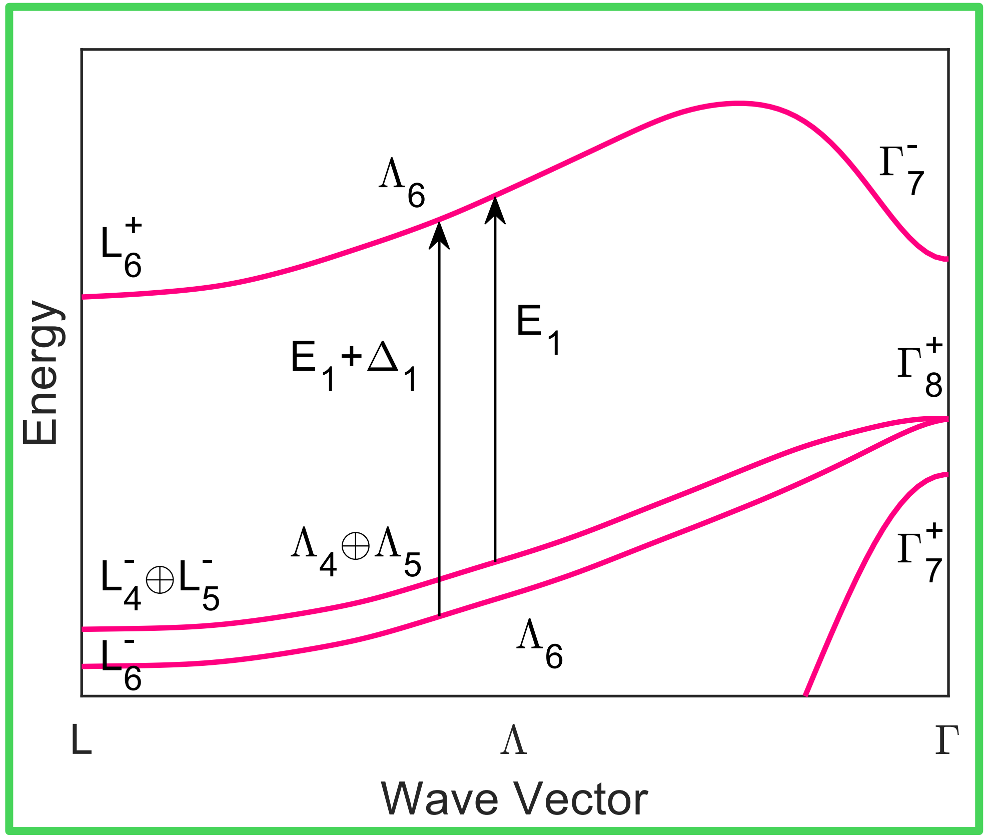

Basis:

$$L_6^+: |Z\uparrow\rangle, |Z\downarrow\rangle$$

$$L_4^-\oplus L_5^-: \frac{1}{\sqrt{2}}|(X+iY)\uparrow\rangle, \frac{1}{\sqrt{2}}|(X-iY)\downarrow\rangle$$

$$L_6^-: \frac{1}{\sqrt{2}}|(X+iY)\downarrow\rangle, \frac{1}{\sqrt{2}}|(X-iY)\uparrow\rangle$$

P. Yu, M. Cardona, *Fundamentals of Semiconductors* (Springer, Berlin, 1996).
E. O. Kane, J. Phys. Chem. Solids **1**, 249 (1957).

L-valley non-parabolicity and extra terms

From $\boldsymbol{k}\cdot\boldsymbol{p}$ theory and for small $k_\perp$ in the L-valley (parabolic approximation):

$$E_{\mathrm{CB}}(k_\perp) = E_1 + \frac{\hbar^2 k_\perp^2}{2m_0}\left(1 + \frac{\bar{P}^2}{m_0}\left[\frac{1}{E_1} + \frac{1}{E_1+\Delta_1}\right]\right),$$

$$E_{\mathrm{hh}}(k_\perp) = \frac{\hbar^2 k_\perp^2}{2m_0}\left(1 - \frac{\bar{P}^2}{m_0 E_1}\right),$$

$$E_{\mathrm{lh}}(k_\perp) = -\Delta_1 + \frac{\hbar^2 k_\perp^2}{2m_0}\left(1 - \frac{\bar{P}^2}{m_0(E_1+\Delta_1)}\right).$$

E_1 and $E_1+\Delta_1$ transitions happen over a $k_{\max}$, not just at the L-valley.

Extra $k_\perp$ terms of the matrix element E_P in the Λ-direction increase $\mu_\perp^{(E_1)}$ and increase $\mu_\perp^{(E_1+\Delta_1)}$.

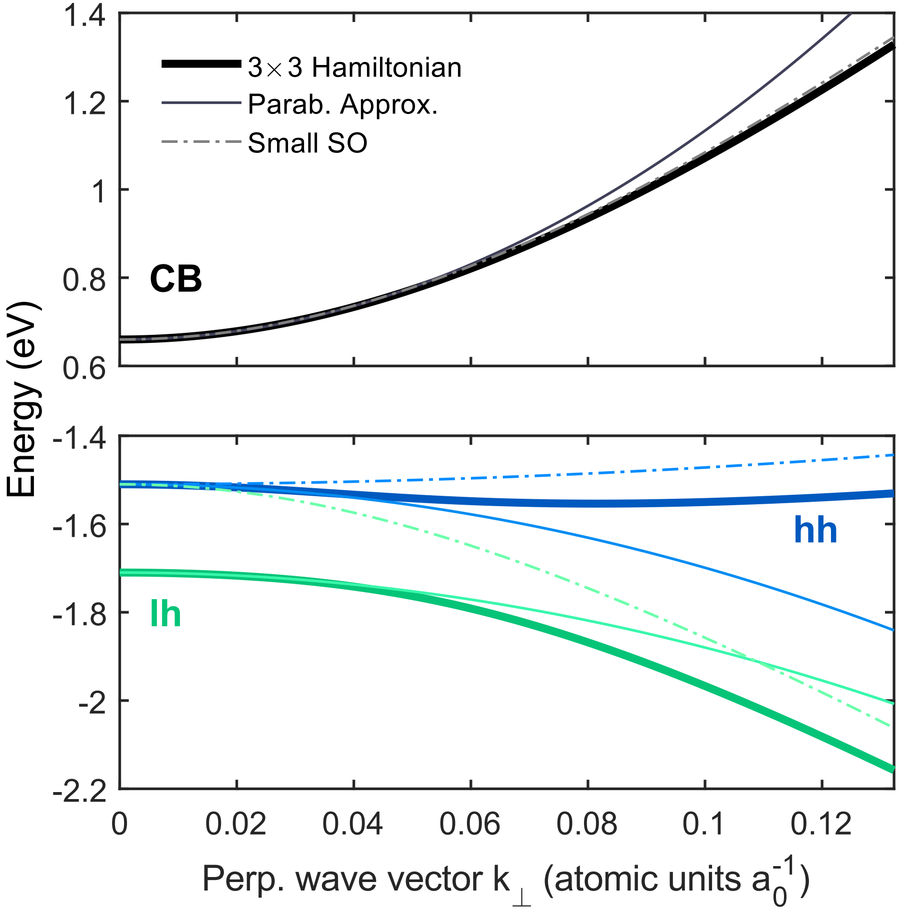

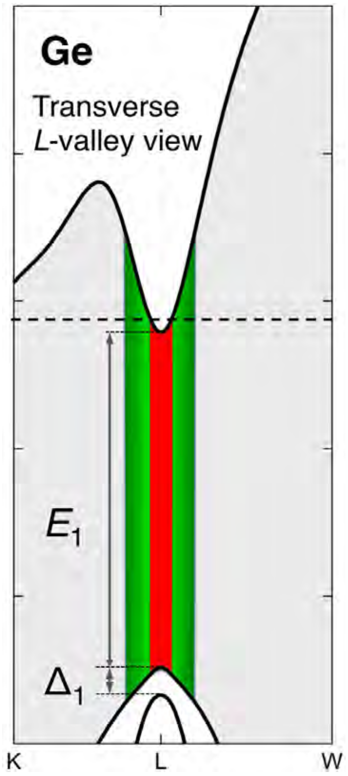

C. Xu *et al.*, Phys. Lett. **118**, 267402 (2017).
M. Cardona, Phys. Rev. B **15** 5999 (1977).

Charge carrier concentration

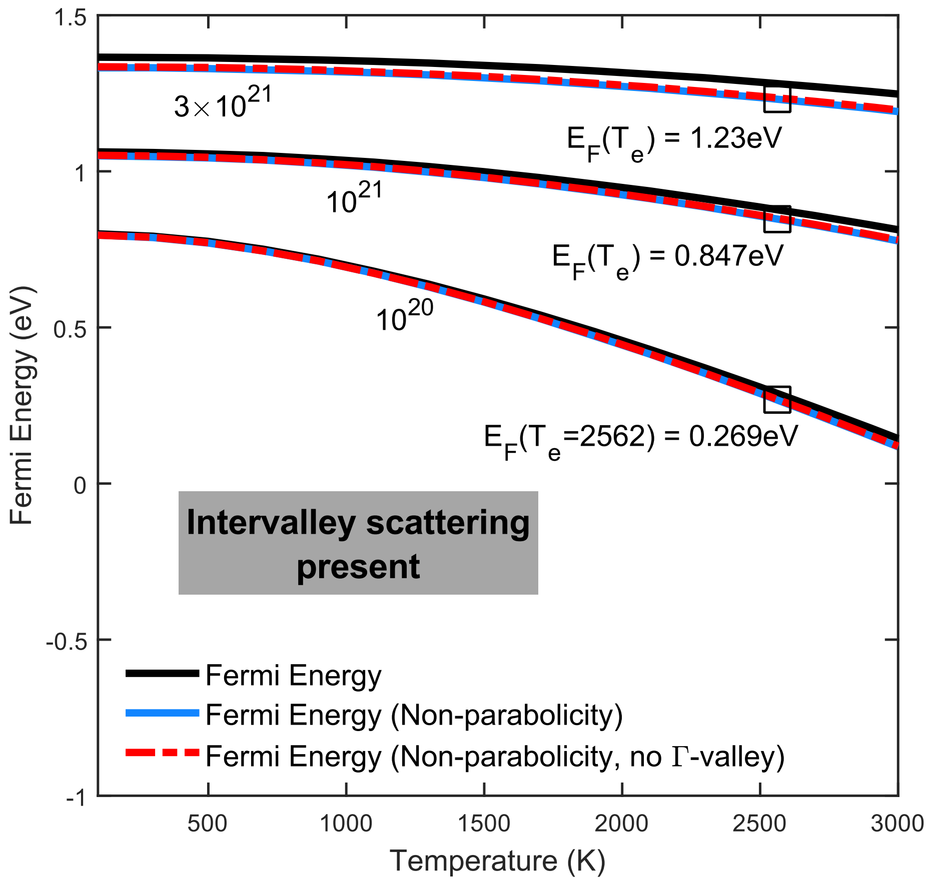

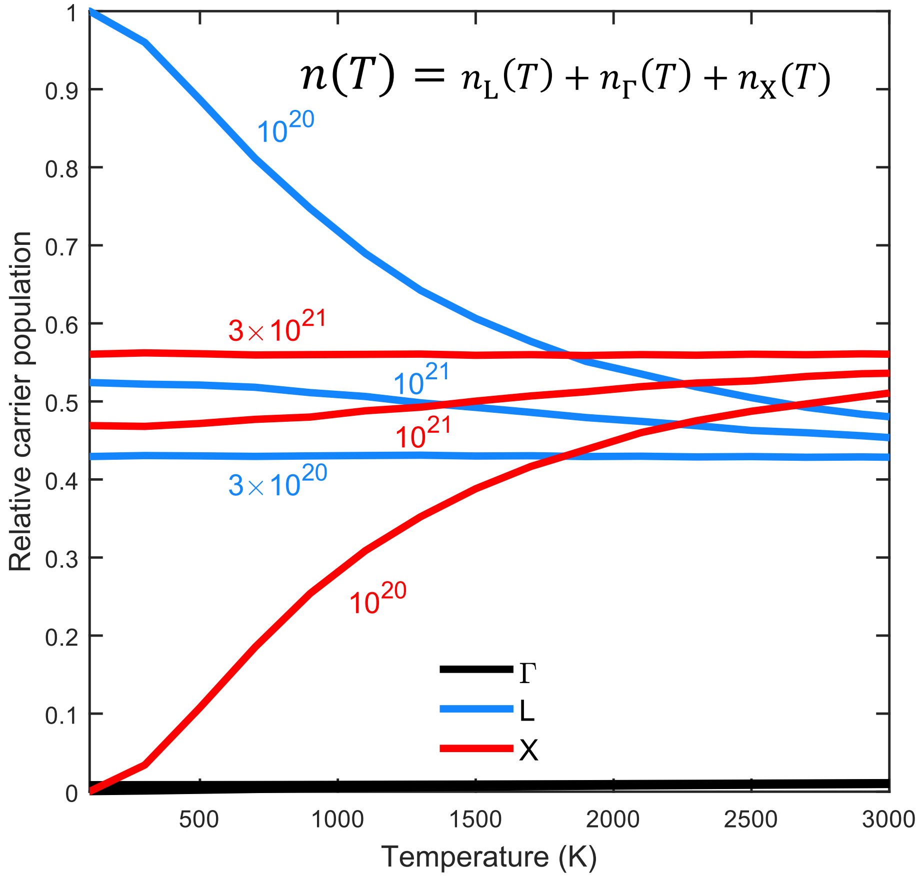

Temperature of carriers

Carrier temperature can be calculated by setting the absorbed optical energy equal to the electron-hole distribution:

$$\sum_{\mathrm{C}}\sum_{\vec{k}} E^{\mathrm{C}}\left(\vec{k}\right) f_e\left(\vec{k}\right) + \sum_{\mathrm{V}}\sum_{\vec{k}} E^{\mathrm{V}}\left(\vec{k}\right) f_h\left(\vec{k}\right) = n\hbar\omega,$$

Which approximates to:

$$T \approx \frac{1}{3k_{\mathrm{B}}}\left(\hbar\omega - E_{\mathrm{ind}}\right)$$

A. L. Smirl, The physics of nonlinear absorption and ultrafast carrier relaxation in semiconductors. (1980).